Genome-wide association analysis of resistance to scald in an adapted multiparent winter malting barley population

J.M. Kolkman[1,2,*], S.S. Sepp[1], K. Kunze[1], G.C. Bergstrom[2], and M.E. Sorrells[1]

Affiliations

[1] Plant Breeding and Genetics Section, School of Integrative Plant Science, Cornell University, Ithaca, NY, USA

[2] Plant Pathology and Plant-Microbe Biology Section, School of Integrative Plant Science, Cornell University, Ithaca, NY, USA

*Corresponding Author: Judith M. Kolkman (jmk87@cornell.edu)

Core Ideas

- Resistance to scald in a large multiparent population was derived from a major resistance gene (*Rrs1*) and several smaller effect QTLs
- *Rrs1* resistance was derived from 'Lightning' and is located within a large linkage block on Chromosome 3H
- Fewer days to heading and taller plants were correlated with less disease in the multiparent winter malting barley population in NY state
- A QTL for resistance to scald co-localized on chromosome 2H with winter survival, heading date, and plant height
- FarmCPU was an optimal model for association analysis for resistance to scald in the multiparent unbalanced diallel population.

ABSTRACT

Scald, caused by the fungus *Rhynchosporium graminicola* Heinsen 1897, is a major foliar disease in winter malting barley (*Hordeum vulgare* L). Resistance to scald in winter malting barley is controlled by major and minor resistance genes. We used a population of 377 lines derived from biparental crosses among five winter malting barley parents to analyze resistance to scald and associated agronomic traits. Increased winter survival and later heading dates were negatively correlated with increased resistance, whereas increased height was positively correlated with resistance. A genome-wide association study (GWAS) for resistance to scald was analyzed with multiple models, using 14,789 SNP and 374 lines. The similarities and differences between the models were identified in SNP trait associations and phenotypic effect sizes. SNP associations identified a large region on chromosome 3H across models. FarmCPU identified additional associations on chromosomes 2H, 3H, 4H and 7H. Linkage disequilibrium on chromosome 3H and GWAS for resistance to scald using the *Rrs1*-linked marker, HVS3, as a covariate confirmed *Rrs1* was segregating in this population. GWAS for winter survival, heading date and plant height identified associations across the genome, with chromosome 2H showing SNP-trait colocalizations between resistance to scald, winter survival, heading date and plant height. Breeding for durable resistance to scald in winter malting barley can include pyramiding major resistance loci, such as *Rrs1*, as well as QTL for disease resistance and agronomic traits.

PLAIN LANGUAGE SUMMARY

Genetic architecture of resistance to scald in winter malting barley

Scald is an important foliar pathogen in winter malting barley, affecting both grain yield and quality. While resistance to scald is controlled by major and minor resistance genes, agronomic traits are also known to limit the spread of scald in barley. We determined the genetic architecture using a large multiparent population of winter malting barley. The FarmCPU genome-wide association model proved

46 optimal for defining the resistance genes, with the major resistance gene, *Rrs1*, conferring 29% of the
47 variation in this population. Fewer days to heading and taller plants contributed to plant avoidance of
48 scald. Reduced canopy coverage in plants with low winter survival led to less scald severity. A region of
49 the genome contributing a minor resistance effect was co-localized with a region for plant height,
50 heading date and winter survival.

51

52 **Abbreviations**

53 BLINK, Bayesian-information and linkage-disequilibrium iteratively nested keyway
54 DH, doubled haploid
55 DLA, diseased leaf area
56 FarmCPU, fixed and random model circulating probability unification
57 GAPIT, genome association and prediction integrated tool
58 GWAS, genome wide association study
59 HT, height
60 LD, linkage disequilibrium
61 LRR-RLK, leucine-rich repeat receptor-like proteins
62 MAF, minor allele frequency
63 MAGIC, multiple advanced generation inbred cross
64 MTA, marker trait association
65 MLM, mixed linear model
66 MLMM, multiple loci mixed linear model
67 PCA, principal components analysis
68 RIL, recombinant inbred line
69 SNP, single nucleotide polymorphism

70 QTL, quantitative trait loci

71 PEI, pectin esterase inhibitor

72 QQ, quantile-quantile

73 Reml, restricted maximum likelihood model

74 SCAR, sequenced characterized amplified region

75 PVE, phenotypic variation explained

76 WS, winter survival

77

78 **1 INTRODUCTION**

79 Barley, *Hordeum vulgare* L., is a globally important crop used for livestock feed, human food, and for
80 malt used in brewed and distilled beverages. The increased demand for malting barley by the craft
81 brewing industry has led to increased malting barley production in non-traditional barley growing
82 regions (Shrestha & Lindsey, 2019). The adoption of malting barley in the Northeast US has been
83 fostered by development of improved management recommendations for barley grown in higher rainfall
84 and more humid conditions than in traditional barley growing regions (Shrestha & Lindsey, 2019; Siller et
85 al., 2021). Winter barley offers consistently higher yield and often higher quality than spring barley and
86 often avoids unfavorable spring planting conditions and summer droughts. Along with agronomic
87 management differences, a shift from spring to winter malting barley alters the disease exposure profile,
88 resulting in an environment conducive to the proliferation of scald. Barley scald is a foliar fungal
89 pathogen, that flourishes in the cooler climates reaching up to 77% diseased leaf area of upper canopy
90 during early grain filling stages in susceptible cultivars grown in New York (Kolkman et al., 2025a). Scald
91 can cause both a reduction in quality (Avrova & Knogge, 2012), and yield losses ranging from 10 to 45%
92 (Shipton et al., 1974), and up to 65% in severe epidemics (Beigi et al., 2013).

93 Scald in barley is caused by *Rhynchosporium graminicola* Heinsen 1897 (Crous et al., 2021; formerly
94 known *as R. commune*; Zaffarano, et al., 2011) a hemibiotrophic foliar fungal pathogen that thrives in
95 cooler temperatures (Zaffarano et al., 2008). Originally identified in 1897 (Frank, 1987), *R. graminicola*
96 was renamed as *R. secalis* (Oudem.) J.J. Davis in 1919 (Davis, 1919), renamed again in 2008 as *R.*
97 *commune* to indicate host speciation specific to *Hordeum* species (Zaffarano et al., 2008, 2011).
98 *Rhynchosporium graminicola* is proposed to have originated in the cool climates of Scandinavia
99 approximately 2500 years ago as a host jump from an unknown grass species (Brunner et al., 2007).
100 *Rhynchosporium graminicola* spreads through previously infected barley debris and/or infected seed
101 (Ababa et al., 2023). Conidia land on leaf surfaces and produce a germ tube along the intercellular
102 grooves that produces an appressorium that penetrates through the cuticle, all within the first 24 hours
103 of exposure (Linsell et al., 2011). Hyphae grow below the cuticle, above the anticlinal walls and between
104 the epidermal cells, between the pectin layer and outer cell wall, disrupting the pectic layer and cuticle
105 for pectin degradation (Ayesu-Offei & Clarke, 1970; Ryan & Grivell, 1974; Lehnackers & Knogge, 1990;
106 Linsell et al., 2011). The cuticle and epidermal layers separate with the production of a packed hyphal
107 mat, forming a subcuticular stroma, inducing a water-soaked lesion, all within approximately 4 to 8 days
108 (Ayesu-Offei & Clarke, 1970; Linsell et al., 2011). Mesophyll collapse follows approximately 7 to 14 days
109 post inoculation, creating a straw-colored necrotic lesion surrounded by dark brown borders at which
110 point hyphal growth increased, likely due to the release of nutrients from the collapsed mesophyll cells
111 (Ayesu-Offei & Clarke, 1970; Lehnackers & Knogge, 1990; Linsell et al., 2011). Conidia are produced from
112 subcuticular and/or substomatal stroma, which protrude through the cuticle along the leaf surface.

113 Resistance to scald in barley has been attributed to both major resistance genes and quantitative trait
114 loci (QTLs; as reviewed by Zhang et al., 2020). In total, 11 major resistance genes have been described
115 (as compiled by Noe et al., 2025) with major resistance genes located on all chromosomes except
116 chromosome 5H. Several of the *Rrs* genes are comprised of multiple alleles and/or loci, such as the *Rrs1*

117 gene complex located on chromosome 3H that includes the previously described alleles *Rh*, *Rh1*, *Rh3*
118 *Rh4* and *Rh7* (Bjørnstad et al., 2002). While no causal gene underlying the *Rrs* genes has been
119 determined, several *Rrs* genes have been fine-mapped. The *Rrs1* gene region has been delimited to a
120 region of 0.8 Mbp with 10 candidate genes using the Morex genome sequence. The *Rrs1* gene is not,
121 however, present in the Morex genome, and is hypothesized to be presence-absence and/or a gene
122 duplication variant. There are several candidates that are plausible in this genomic region that is reticent
123 to recombination, due to its centromeric location, including a protein kinase (Looseley et al., 2020). The
124 *Rrs2* resistance gene is proposed to be in a cluster of pectin esterase inhibitor (PEI) genes, either as a
125 unique gene, a combination of PEI genes and/or other unidentified gene(s) (Marzin et al., 2016). The
126 *Rrs13* resistance gene, fine-mapped within a 0.58 to 1.2 Mbp region, codes for two to seven tandemly
127 repeated leucine-rich repeat receptor-like proteins (LRR-RLP) and a lectin receptor-like kinase (Eckstein
128 et al., 2024). More recently, the *Rrs18* gene has been identified upstream of *Rrs13* (Coulter et al., 2019).
129 Fine-mapping and RNA expression analysis identified four candidate genes with the most likely candidate
130 gene a serine/threonine protein kinase. As well as these four genes, a stable QTL for adult plant
131 resistance to scald, QSc.VR4, was fine-mapped to a 0.38 Mbp region that included an LRR-RLK multi-gene
132 family, and a germin-like protein multigene family (Wang et al., 2020).

133 Numerous genome-wide association studies (GWAS) have been utilized to identify and characterize
134 resistance to scald in barley. Association studies have relied on a variety of populations, including
135 diversity panels (Looseley et al., 2018; Hiddar et al., 2023; Kunze et al., 2024; Noe et al., 2025), a multiple
136 advanced generation inbred cross (MAGIC) population (Hautsalo et al., 2021), the HEB25 nested
137 association mapping population (Büttner et al., 2020), and a variety of populations that included diverse
138 germplasm, including landraces, wild species and breeding lines (Looseley et al., 2018, 2020; Clare et al.,
139 2023; Ababa et al., 2024; Ijaz et al., 2024). Many trials utilize greenhouse trials to ascertain seedling
140 resistance (major gene resistance), using one or more isolates to characterize resistance to specific

141 isolates. Several studies relied on (natural) field infection to identify adult plant resistance (Daba et al.,
142 2019; Looseley et al., 2020; Ijaz et al., 2024). All GWAS studies used spring barley, except for two studies
143 that used spring, winter and/or facultative barley lines (Looseley et al., 2020; Kunze et al., 2024). Adult
144 plant resistance in the field encompasses natural infection, and resistance comprised of major resistance
145 (*Rrs*) genes and/or QTL for resistance to scald. Adult plant resistance has been associated with genes
146 coding for plant growth traits, such as *sdw1*, the gibberellin 2-oxidase gene, *HvGA20ox2* (Xu et al., 2017),
147 implicated with plant height and susceptibility to scald (Looseley et al., 2018). Improving barley for
148 resistance to scald relies on agronomic practices as well as breeding for resistance. Due to the potential
149 for *R. graminicola* populations to overcome resistance (Mcdonald, 2015; Ababa et al., 2024),
150 understanding the facets of resistance is imperative in breeding for sustainable resistance.

151 Genome wide association studies are useful for the identification of marker-trait associations and
152 characterization of trait architecture across the genome. The premise of GWAS relies on maximizing
153 meiotic recombination events by utilizing populations consisting of a large diverse number of genotypes
154 in conjunction with high SNP marker density, and in many cases, using population structure and kinship
155 to minimize false positive results (Flint-Garcia et al., 2005; Yu et al., 2006). Several models of GWAS have
156 been developed that use different approaches to identify marker trait associations (Tibbs Cortes et al.,
157 2021). In contrast, breeding programs are targeted to regional adaptation and are generally limited to
158 elite material based on founders and the introgression of adapted material that may have originated
159 from diverse or pre-breeding efforts (Kelly et al., 1998). Large populations are created with the goal of
160 finding the transgressive segregants that move crop development and the release of novel cultivars
161 forward.

162 In this study we characterized resistance to scald in an unbalanced diallel breeding population of winter
163 malting barley recombinant inbred lines and doubled haploids derived from biparental crosses between
164 five founder lines that are adapted to New York environments. We examined the correlation of

agronomic traits, such as winter survival, days to heading and plant height with resistance to scald as a means of escape and/or avoidance mechanisms. Using GWAS, we characterized the genetic architecture of resistance to scald in the multiparent population, and the co-localization of SNP associations between resistance to scald and winter survival, heading date and plant height. We explore a suite of GWAS models available in GAPIT version 3 (Wang & Zhang, 2021) to determine the appropriate GWAS model for the multiparent unbalanced diallel population, given the relatedness and limited meiotic recombinant events between lines within the germplasm.

2 MATERIALS AND METHODS

2.1 Germplasm and trait phenotyping

2.1.1 Plant germplasm

A population of 377 winter malting barley breeding lines was derived from an unbalanced diallel mating design using four winter malting barley cultivars, including 'Flavia', , 'KWS Scala', 'SY Tepee', and 'WintMalt' and one facultative malting barley cultivar ('Lightning'; Hayes et al., 2021). F_1 plants from the corresponding 10 cross combinations were advanced to the F_5 stage through single seed descent and/or creation of doubled haploids resulting in 183 recombinant inbred lines (RILs) and 194 doubled haploid (DHs) lines (Figure 1) for a total of 377 lines (Figure 1). The largest number of lines was derived from 'Lightning' x 'SY Tepee' crosses, with 93 lines. 'Lightning' was the parent with the most lines represented, with 272 (72%) of the 277 lines. 'WintMalt' was the parent with fewest lines represented with only 95 of the 377 lines (25%). The fewest number of lines were from the cross between 'WintMalt' x 'SY Tepee', with four lines. Additional parents were present in the population with 43.8% (165 lines), 35% (132 lines), 26% (100 lines) for 'SY Tepee', 'Flavia', and 'KWS Scala' respectively.

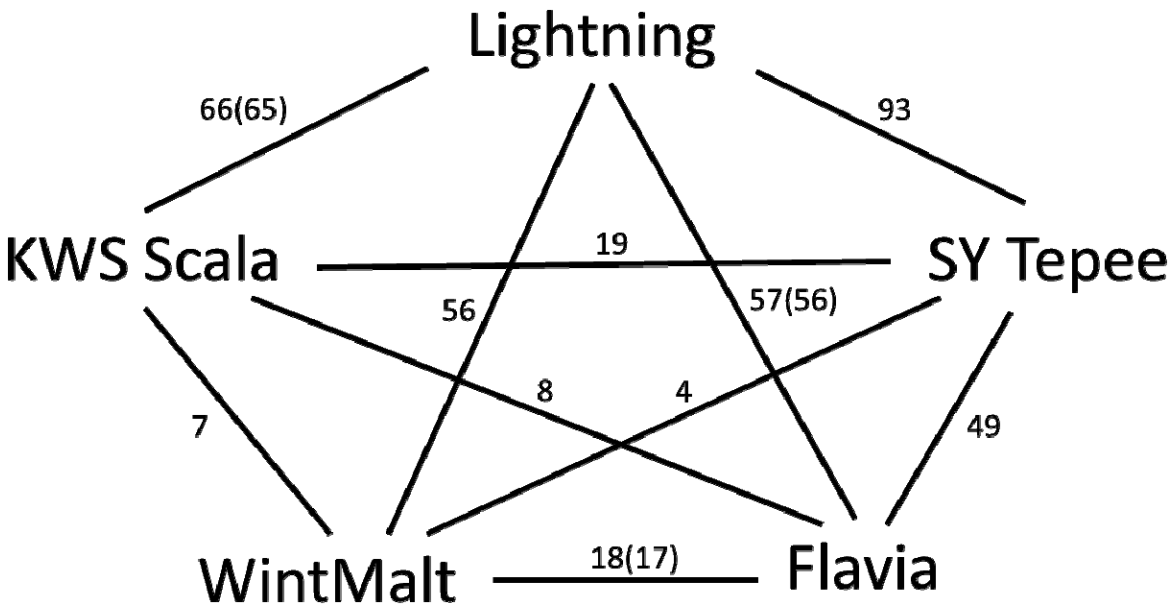

Figure 1. Structure of the unbalanced diallel multiparent population derived from five adapted cultivars. The 377 lines consisted of recombinant inbred lines and doubled haploids. The number of lines between each biparental cross is indicated along the line between the two parents, which were used for statistical analysis (377 lines) and for GWAS analysis (374 lines) with three lines less as indicated by the numbers in parenthesis.

2.1.2 Field trials

The diallel population was planted in four field sites (environments) at the Cornell University Campus Area Farms in Tompkins County near Ithaca, New York and included the Snyder Farm and Helfer Farm field sites in 2022, and the McGowan Farm and Ketola Farm field sites in 2023. Trials were grown in an augmented design with a single replication in each environment and included the parental cultivars as well as check cultivars ('KWS Scala', 'Lightning' and 'Endeavor') within four blocks in both 2022 environments (Snyder Farm and Helfer Farm), and within eight and ten blocks in Ketola Farm and McGowan Farm field sites in 2023, respectively. Seeds were planted in plots with 1.2 m width, 3.0 m

200 plot length, with a 17.8 cm space between rows within the plot and 25.4 cm between plots. No plant
201 growth hormone or foliar fungicides were applied. Preplant fertilizer of 10:10:10 was applied at 224
202 kg/ha (22.4 kg ha^{-1} N) and followed by a top dress in the spring of 67 kg ha^{-1} N via liquid Urea-ammonium
203 nitrate 30. The spring applied herbicide regime in 2022 consisted of Harmony (35 g ha^{-1}), bromoxynil
204 (BROX-2-EC at 1.5 L ha^{-1}) and Induce surfactant (0.7 L ha^{-1}). Herbicide applications in the spring of 2023
205 consisted of Axial XL (1.2 L ha^{-1}), Harmony Extra SG (35 g ha^{-1}) and Induce surfactant (0.7 L ha^{-1}). No foliar
206 fungicide was applied.

207 **2.1.3 Trait phenotyping**

208 Scald infections relied on the natural inoculum present at each field site. *A priori* knowledge of these
209 field sites indicated a historical presence of the scald pathogen in each environment. The scald
210 susceptible cultivar 'KWS Scala' (Blachez et al., 2018) was planted in each block of each experiment and
211 acted as a susceptible check and spreader ensuring adequate conidial inoculum across the trial. Plots
212 were scored for scald symptoms at approximately Feekes stage 11.1 to 11.3 on June 13th and 9th in
213 2022 at the Helfer Farm and Snyder Farm field sites, respectively, and at Feekes stage 11.1-11.3 from
214 June 26th to the 30th, and June 15th to 19th in 2023 at the McGowan Farm and Ketola Farm field sites
215 respectively. Plots were scored on a 0-9 scale in all four environments. Severity was also scored as a
216 percentage diseased leaf area (DLA) for the upper canopy in 2023. 2022 trial scores were converted to a
217 % DLA. Additional agronomic traits were scored in the trials including winter survival (WS), measured as
218 percentage of plants surviving taken in the early spring; heading date (HD), when 50% of the heads had
219 completely emerged from the sheath (converted to Julian heading date); and plant height, measured as
220 the height (HT) from the ground to the top of the spike excluding awns.

221

222

223 **2.1.4 Data analysis**

224 The scald DLA, WS, HD and HT were analyzed separately in 2024 JMP® 17.1 (JMP Statistical Discovery
225 LLC, Cary NC) using a mixed model (restricted maximum likelihood; Reml) with genotype as fixed effects,
226 and environment, row within environment, and column within environment as random model effects.
227 Least squared means were used to determine frequency distributions and parental phenotypic value in
228 comparison to the population. Spearman's correlations between DLA, WS, HD, and HT were determined
229 using JMP. Heritability was determined on an entry-means basis where $h^2 = \sigma^2_g/(\sigma^2_e/t+ \sigma^2_g)$, with σ^2_g,
230 and σ^2_e representing genetic variance, and experimental error, respectively, and t representing number
231 of test environments (Fehr, 1987).

232 To normalize the residuals and homoscedasticity for association analysis, the DLA, WS, HD, HT
233 measurements were analyzed in a simple linear model in R to estimate the residual parameters for the
234 population of 377 without controls, with model effects of genotype, environment, row within
235 environment and column within environment as fixed effects. A constant of 1 was added to each DLA
236 measurement to avoid nulls for transformation. The best lambda for transformation of the data was
237 determined using the Box-Cox function (Box & Cox, 1964) in the MASS package in R v3.2.3 (R Core Team,
238 2015), that was used to transform for normal residuals and homoscedasticity. The DLA (with added
239 constant of 1), WS, HD and HT were transformed using respective lambda values of -0.1818, 2.9494, -
240 7.0303 and 0.0606 for DLA, WS, HD and HT, respectively. The HD transformed data was multiplied by 1 x
241 10^{16} for further analysis.

242 The best linear unbiased predictors (BLUPs) transformed DLA scores were estimated using Reml in JMP
243 with WS, HD and HT as fixed covariate effects and genotype, environment, row within environment, and
244 column within environment as random effects. The BLUPs for the transformed values for DLA, WS, HD,

245 and HT were also calculated using Reml in JMP with genotype, environment, row within environment
246 and column within environment as random effects.

247 2.2 Genotypic Analysis

248 2.2.1 SNP Genotypic Data

249 Plant tissue was harvested from the multiparent population at the two-leaf stage. Tissue was lyophilized
250 and a modified Cetyltrimethylammonium bromide (CTAB) extraction was used for DNA extraction (Doyle
251 & Doyle,1987). DNA was genotyped with the 50K Illumina iSelect SNP array (Bayer et al., 2017; Mascher
252 et al., 2017, 2021) at the USDA-ARS North Central Small Grains Genotyping Lab in Fargo, ND and
253 resulted in high quality SNP data for 374 lines. The SNP data was trimmed from the original 43,078 SNPs
254 to exclude homozygous SNPs across the population using TASSEL 5.0 (Bradbury et al., 2007). The 15,463
255 SNPs were used to estimate population structure.

256 2.2.2 Marker Genotypic Data

257 Leaf tissue was collected for specific marker traits associations (MTA) within known resistance and/or
258 height genes. For the MTA analysis, three kernels per line included in the multiparent population were
259 planted in a 96 cell tray and grown under a light bench. Tissue was harvested at the seedling stage and
260 lyophilized. The modified CTAB extraction was used to extract DNA (Doyle & Doyle, 1987).

261 The multi-parent population was genotyped for the plant height gene, *HvGA20ox2*, also known as *semi-*
262 *dwarf1* (*sdw1*), to test for the presence of the *sdw1.d (Diamant)* or *sdw1.c* (denso) alleles (Xu et al.,
263 2017). The *sdw1.d* and *sdw1.c* alleles were amplified via polymerase chain reaction using mutant
264 specific primers based on Xu et al. (2017), with the adaptation of a fluorescent M13-tail in the forward
265 primers for both the sdw1.d allele (5401F_M13F; 5'- TGTAAAACGACGGCCAGTGGTGCTCCAGACCGCTCAG-
266 3') and sdw1.c (MC40861P3F_M13F; 5'- TGTAAAACGACGGCCAGTTATGGCGTGACCAAAGGTTC-3') that

267 correspond to the reverse primers for *sdw1.d* (5549R; 5'-CGGCGGAGGGGTCAATG-3'), and *sdw1.c*
268 (MC40861P4R; 5'- CACCAATCCACCACGAAGA-3'). The PCR reaction consisted of ~30 ng genomic DNA,
269 12.5 µl of GoTaq polymerase, 0.8 µM M13F primer, 6 µM R primer, 6 µM M13-FAM primer (*sdw1.d*) or
270 M13-VIC primer (*sdw1.c*) and 8.22 µl of H_20 in a 25 µl reaction. The PCR amplification protocol for the
271 *sdw1.d* primer pair included an initial denaturation step of 94°C for 3 m, 30 cycles (94°C for 1 m, 55°C for
272 30 s, 72°C for 30 s), 10 cycles (94°C for 1 m, 50°C for 30 s, and 72°C for 30 s), and a final extension cycle
273 of 72°C for 20 m. The PCR amplification cycle for the sdw1.c was similar to above, however the
274 annealing temperatures in the two cycles were 54°C and 53°C. Fragment analysis was performed on
275 pooled samples by the Biotechnology Resource Center (BRC) Genomics Facility (RRID:SCR_021727) at
276 the Cornell Institute of Biotechnology (*http://www.biotech.cornell.edu/brc/genomics-facility*) on an
277 Applied BioSystems 3730xl (Thermo Fisher Scientific, Waltham, MA), with the ABI 500LIZ size standard.
278 Results were analyzed in Genemarker (SoftGenetics, LLC, State College, Pennsylvania).

279 In addition, the HVS3 SCAR marker (Genger et al., 2003) was screened in the parental lines and
280 multiparent population using ~20ng genomic DNA, 1X GoTaq ® Green Master Mix (Promega
281 Cooperation, Madison, WI), 5µM Forward primer (5'-AAT CCT ACC TAT CCC ACC TT-3'), 5 µM Reverse
282 primer (5'-TAT TTT CAG CCT TGT TCG GC-3') in a final reaction volume of 25 µl. The DNA was amplified
283 via PCR using an initial step of 94°C for 3 m, 35 amplification and extension cycles (94°C for 30 s, 50°C for
284 30 s, 72°C for 1 m), followed by a final extension cycle of 72°C for 20 m. The PCR products were
285 amplified on a 2% agarose gel using GelRed ® Nucleic Acid Stain (Biotium, Inc, Freemont, CA) for
286 verification of PCR on a UV lightbox.

287 ## 2.3 Genome-wide association analysis

288 ### **2.3.1 Genome-wide association mapping for resistance to scald with multiple models**

289 Association analysis was used to identify regions of the genome that conferred resistance to the scald
290 pathogen in our adapted germplasm. Phenotypic data included the transformed DLA, WS, HD and HT
291 BLUPs. Of the diallel population, 374 lines were used that included both genotypic and phenotypic data.
292 The 43,078 SNPs (Morex version 3) derived from the 50K Illumina iSelect SNP array (Bayer et al., 2017;
293 Mascher et al., 2017, 2021) were filtered to exclude homozygous SNPs across the population in TASSEL
294 5.0 (Bradbury et al., 2007).

295 Genome-wide association for Box-Cox transformed DLA BLUPs for scald that included WS, HD and HT as
296 covariates as previously described was ascertained using GAPIT version 3 (Wang & Zhang, 2021) in R
297 Studio (RStudio 2025.09.1+401, Posit Software, PBC). The Mixed Linear Model (MLM), Multiple Locus
298 Mixed Linear Model (MLMM), Fixed and random model Circulating Probability Unification (Farm CPU)
299 and (Bayesian-information and Linkage-disequilibrium Iteratively Nested Keyway (BLINK) models (Yu et
300 al., 2006; Zhang et al., 2010; Segura et al., 2012; Liu et al., 2016; Huang et al., 2019), using the 14,789
301 SNPs, were used to estimate marker trait association parameters for resistance to scald. Kinship and
302 principal component analysis (PCA) were determined within GAPIT version 3 to be used in the
303 appropriate models. The Bonferroni threshold (Bonferroni, 1936) was used as an initial default
304 significance threshold for R^2 (MLM) and Percent Variation Explained (PVE; MLM, MLMM, FarmCPU, and
305 BLINK). The resulting Quantile-Quantile (QQ) plots and contributing PVE were examined to determine
306 the appropriate GWAS model for this structured population. To reduce Type II false negative errors due
307 to the conservative nature of the Bonferroni threshold, the QQ plots were examined to determine the
308 best GWAS fit that combined the reduction of spurious associations and putative significant or strong
309 associations. The MLMM, FarmCPU and BLINK GWAS model QQ plots showed a *p*-value differentiation
310 at the $-\log_{10}(p) = 4.0$. To determine the appropriate R^2 (MLM only) and PVE (MLM, MLMM, FarmCPU and
311 BLINK models) the 'N.sig = n' prompt was used in GAPIT version 3 for the significance threshold where 'n'
312 equals the number of markers for each model equal or above the $-\log_{10}(p) = 4.0$ threshold. An additional

313 association analysis using FarmCPU with PCA = 3 as a covariate was used to validate model selection with
314 or without PCA.

315 **2.3.2 The *Rrs1* gene complex**

316 Linkage disequilibrium (LD) surrounding the two strongest SNP associations identified on chromosome
317 3H at 174 Mbp and 442 Mbp were analyzed to determine if they were the same peak or independent
318 associations. The LD was first assessed in TASSEL 5.0 (Bradbury et al., 2007) between the SNP at 174
319 Mbp and all the other SNPs on chromosome 3H (Figure 3A), and between the SNP at 442 Mbp and all
320 the other SNPs on chromosome 3H. The Manhattan plots for the GWAS MLM model (Figure 2) were
321 overlaid with LD estimates and used to confirm the presence of a large linkage block across the
322 centromeric region of chromosome 3H, as visualized in the 'ggplot2' package of R v3.2.3 (R Core Team,
323 2015). The GWAS MLM model was used to assess associations using GAPIT version 3, using the same
324 methodology as above, except for only using the 354 lines in the GWAS model and using the HVS3
325 marker data as a covariate (Figure 3C).

326 **2.3.3 GWAS for resistance to scald, winter survival, heading date and plant height**

327 The Box-Cox transformed DLA BLUPS (without WS, HD, and HT as covariates), as well as Box-Cox
328 transformed WS, HD, and HT BLUPs were used as independent trait variables in both MLM and FarmCPU
329 analysis using GAPIT version 3 in RStudio, with the 15,463 SNPs. The significant thresholds were based
330 on visual inspection of the QQ plots of FarmCPU and set to $-\log_{10}(p) = 4.0$. As in the first GWAS analysis
331 listed above, the models were run again using the 'N.sig = n' prompt to determine the correct PVE in
332 GAPIT version 3.

333 The LD along chromosome 2H was compared to the significant SNP in the marker-trait association for
334 resistance to scald, to determine if there was co-localization and/or LD between WS, HD, and HT to
335 resistance to scald. The Manhattan plot was created in ggplot2 to map the LD and SNP marker trait

336 associations from the MLM GWAS model, and included the clustered SNP regions of the WS, HD and HT
337 marker trait associations on the short end of chromosome 2H. Regions around the DLA, WS, HD and HT
338 SNP associations were based on the SNP associations in the MLM model that were at or above $-\log_{10}(p)$ =
339 4.0, as an indicator of the confidence interval for the trait. All Manhattan plots were created using
340 ggplot2 in RStudio.

341 **3 RESULTS**

342 3.1 Segregation for disease and agronomic traits in the multiparent population

343 Distributions of disease and agronomic traits showed transgressive segregation for most traits from the
344 parental lines (Supplemental Table S1). The distribution of scald DLA was skewed towards the y-axis,
345 with 'Lightning' as resistant, 'SY Tepee' as moderately resistant, and 'WintMalt', 'KWS Scala' and 'Flavia'
346 as susceptible to scald (Supplemental Fig1). An analysis of variance indicated significant variation for
347 DLA for genotypes, environment and rows within environment. The means and ranges of disease
348 severity for the 377 lines grown across the locations varied with 50.8% (0-99%) in Helfer Farm, 2022,
349 19.9% (0-99%) in Snyder Farm, 2022, 6.0% (0-90%) in Ketola Farm, 2023, and 19.7% (0-95%) in McGowan
350 Farm, 2023.

351 Across all three agronomic traits, significant variation was identified for genotype, rows within
352 environment, and columns within environment, but not between environments. Across the four
353 environments, WS was skewed towards 100% survival, with 'SY Tepee', 'WintMalt' and 'KWS Scala'
354 showing good winter survival (>85%). 'Lightning' and 'Flavia' showed moderate winter survival (~75-
355 80%), while a check cultivar, 'Endeavor', showed poor winter survival. The average winter survival within
356 the population ranged from 75% (Helfer Farm, 2022) to 87% (Ketola Farm, 2023) with an average across
357 the four environments of 79.9%. Differences in heading date between the parents ranged from ~143
358 days (Flavia) to ~151 days ('WintMalt'), with 'Lightning', 'SY Tepee' and 'KWS Scala' showing mid-range

heading dates between 145 days to 147 days. The heading date (Julian) ranged from an average of 142 days in McGowan Farm, 2023 to 150 days to heading in Helfer Farm, 2022. Plant height ranged from an average of 52 cm to 67 cm in Ketola Farm, 2023 (Supplemental Table S1 & S2). Heritability based on an entry-means basis for DLA, WS, HD and HT were 0.76, 0.69, 0.83 and 0.57 respectively.

3.2 Scald is correlated with agronomic traits

Correlations between scald DLA and agronomic traits were ascertained to determine the effect of winter survival, heading date and plant height on scald using the 377 lines in the multiparent population (Supplemental Table S2). A highly significant negative correlation was identified between DLA and plant height ($P < 0.0001$; $R^2 = -0.29$), indicating that taller plants had less disease in the upper canopy. A significant correlation was also identified between heading date and scald DLA ($P < 0.0107$; $R^2 = 0.13$), indicating that a later heading date had more DLA. The correlation between winter survival and DLA was not significant across environments ($P = 0.1065$). Notably, there was a significant interaction between winter survival and heading date (P=0.0229; $R^2 = -0.1171$), and a highly significant interaction between WS and plant height (P<0.0001; $R^2 = 0.38$), and no significant correlation between heading date and plant height.

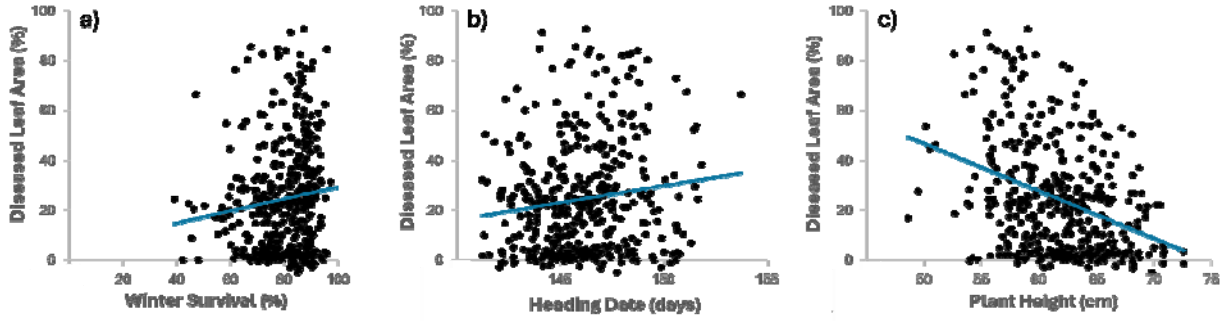

375 Figure 2. Spearman's correlation between resistance to scald (diseased leaf area), and a) winter survival,
376 b) heading date and c) plant height, in the 377 line multiparent population across four environments in
377 2022 and 2023.

378 ## 3.3 Genome wide association mapping for resistance to scald

379 ### 3.3.1 GWAS for resistance to scald using multiple GWAS models

380 Population structure determined via principal component analysis in GAPIT version 3 (Wang & Zhang,
381 2021) indicated that the multiparent population consisted of four groupings with the use of only the first
382 and second PCAs, with the top 3 PCA's accounting for 34% of the genetic variation, indicative of the
383 relatedness between RILs and DHs (Supplemental Figure S2). The QQ plot of the MLM GWAS model
384 showed marked deviation of the observed from expected *p*-values for the MLM model that accounts for
385 both population structure and kinship (Figure 3). The MLMM, FarmCPU and Blink models had QQ plots
386 that were largely in line with the observed and expected *p*-values. The FarmCPU model with PCA = 3 as a
387 covariate resulted in a QQ plot with the observed $-\log_{10}(p)$ values skewing towards the x-axis in
388 comparison to the FarmCPU model with no PCA covariate and was not further pursued (Supplemental
389 Figure S3). The Bonferroni threshold of $-\log_{10}(p) = 5.5$ was initially used in GAPIT version 3 as the default
390 to determine significance. Analysis of the QQ plots, and particularly the QQ plots from the FarmCPU
391 analysis, showed that a threshold of $-\log_{10}(p) = 4.0$ was more appropriate and reduced Type II errors,
392 where the observed veered from the expected regression line. Re-analysis of the GWAS models for
393 MLM, MLMM, FarmCPU and Blink threshold set to $-\log_{10}(p)$ of 4.0 was used to estimate the appropriate
394 phenotypic variation explained (Table 1) and showed distinct differences between models (Supplemental
395 Table S3 – S7).

396 *MLM:* The mixed linear model, with population structure and kinship included, resulted in 75 SNPs
397 associated with resistance to scald (Figure 3) that localized in two SNP clusters on chromosome 3H

398 spanning a region from 89 Mbp to 449 Mbp. Two peaks across this region were identified as the
399 significant associations, with the most significant SNP association located at 174,868,558 bp, with a -
400 $\log_{10}(p)$ = 7.0 (MAF = 0.44; PVE = 14.6%. The second most significant SNP was the SCRI_RS_221644 SNP
401 located on the second peak at 442,185,927 bp with a -$\log_{10}(p)$ = 6.8 (MAF = 0.47; PVE = 0.0%). Of the
402 top five SNP associations, four were identified near the second peak.

403 *MLMM:* Using MLMM, two SNPs were found to be associated with resistance to scald (Figure 3). The
404 single peak identified was located on chromosome 3H, at 174,868,558 bp, with a-$\log_{10}(p)$ = 10.6 (MAF =
405 0.47; PVE = 22.0%). The second association was identified on chromosome 7H at 443,811,200, with a -
406 logP = 4.0 (MAF = 0.33; PVE = 24.1%).

407 *FarmCPU:* The FarmCPU model identified five SNPs associated with resistance to scald (Table 1). The
408 most significant SNP was located on chromosome 3H at 442,185,927 bp with a -$\log_{10}(p)$ = 14.8 (MAF =
409 0.47; PVE = 22.4%). A second SNP on chromosome 3H was located at 553,228,836 with a -$\log_{10}(p)$ = 5.0
410 (MAF = 0.30; PVE = 15.6%). The SNP association on chromosome 2H was at 18,144,981 bp with a -
411 $\log_{10}(p)$ = 5.2 (MAF = 0.43; PVE = 0.0).Additional SNP associations were identified on chromosomes 4H
412 (MAF = 0.240; PVE = 2.2%) and 7H (MAF = 0.33; PVE = 0.0%). Two additional SNP marker trait
413 associations were identified however both had low MAF and are considered aberrations, including the
414 association on chromosome 6H at 65,635,245 bp (MAF = 0.003; PVE = 0.0%) and on chromosome 5H at
415 329,813,939 bp (MAF = 0.02; PVE = 5.7%). FarmCPU with PCA=3 resulted in a QQ plot with the observed

416

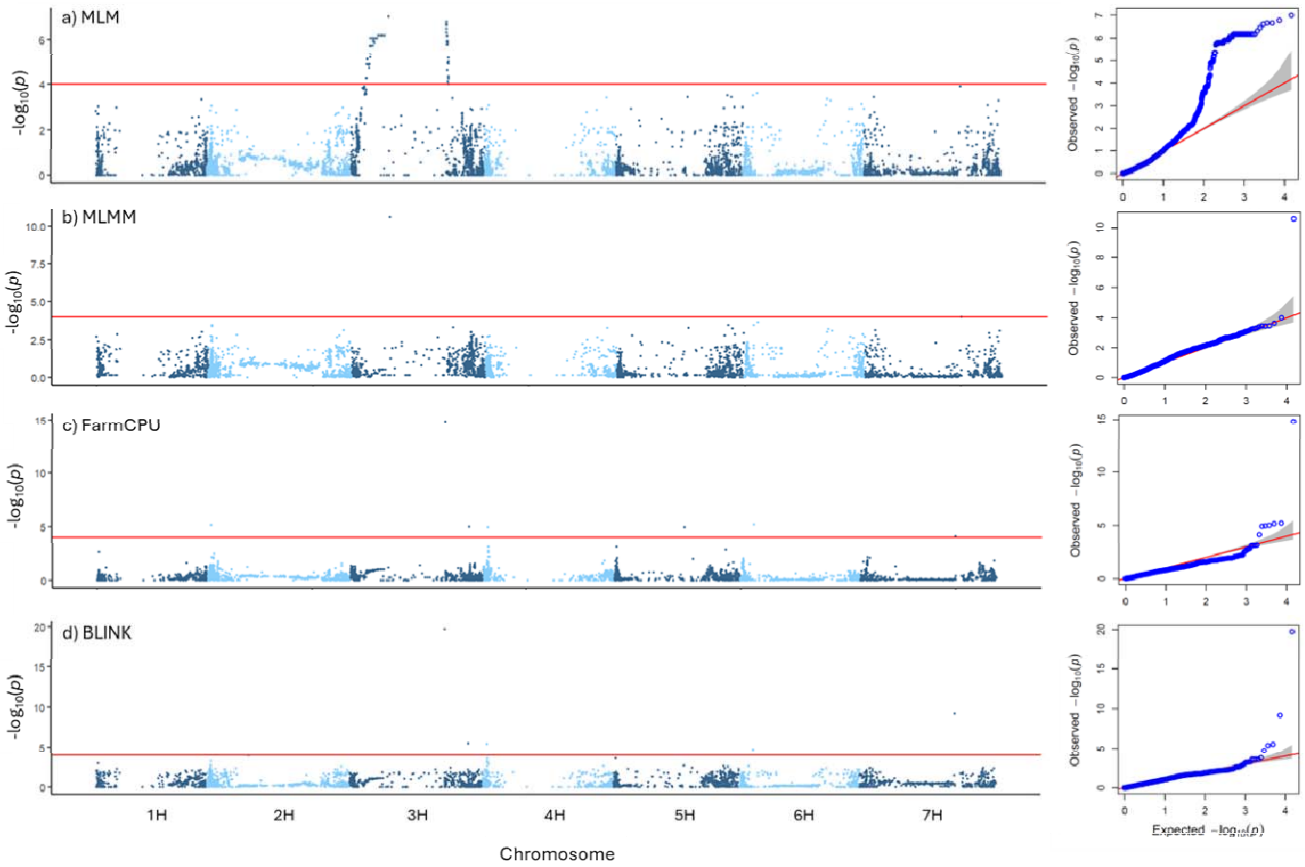

417

418 Figure 3. Manhattan plots of the GWAS models including a) MLM, b) MLMM, c) FarmCPU, and d) BLINK, with corresponding QQ plots (right) in

419 GAPIT version 3 for resistance to scald in the multiparent population with using DLA BLUPs for resistance to scald. DLA BLUPs for resistance to

420 scald were calculated using winter survival, heading date and plant height as covariates in the BLUP model in four environments across 2022 and

421 2023. The red horizontal line in the Manhattan plots indicate the QQ plot - determined threshold of $-\log_{10}(p)$ of 4.0.

422 $-\log_{10}(p)$ values below the expected $-\log_{10}(p)$ values and skewed towards the x-axis and was not
423 considered further (Supplemental Figure S3).

424 *BLINK:* BLINK identified four SNPs associated with resistance to scald. The most significant SNP was
425 located on chromosome 3H: 442,185,927 bp, with a $-\log_{10}(p) = 19.7$ (MAF = 0.47; PVE = 7.3%). The next
426 most significant SNP was located on chromosome 7H: 443,811,200 bp with a $-\log_{10}(p) = 9.2$ (MAF = 0.33;
427 PVE = 6.8%). Other SNP marker trait association included SNPs located on chromosome 3H at
428 553,288,836 bp with a-$\log_{10}(p) = 5.5$ (MAF = 0.30; PVE = 2.7%), and 4H at 22,416,684 bp with a $-\log_{10}(p)$
429 = 5.4 (MAF = 0.24; PVE = 3.3%). As with the FarmCPU model, a SNP association was identified on
430 chromosome 6H: 65,635,245 bp with a $-\log_{10}(p)$ of 4.7 (MAF = 0.003; PAV = 62.3%) and is considered an
431 aberration.

432 A discrepancy between the GWAS models was identified that was important for interpreting how to
433 proceed with the analysis. The difference in SNP marker trait associations between the MLM, MLMM,
434 FarmCPU and BLINK spans both SNP location and effect size. Notably, there appeared to be two large
435 peaks on chromosome 3H (MLM) that were either an association on the first peak (MLMM) or on the
436 second peak (FarmCPU; BLINK). In addition, PVE for the large peaks on chromosome 3H (442 Mbp)
437 varied between MLM (0.0%), FarmCPU (22..4%), and BLINK (7.3%); the corresponding SNP in MLMM at
438 174Mbp (22.0%), indicating the presence of a major gene such as the *Rrs1* co-localizes to that region.

439 Using TASSEL 5.0 (Bradbury et al., 2007), the LD along chromosome 3H was compared to both peaks
440 separately (Figure 4). Using the SNP at 174,868,558 bp, the LD analysis showed that SNPs across both
441 peaks were in LD with the peak at 174 Mbp, indicating a large linkage block that spanned the
442 centromere. The LD analysis comparing the SNPs at the second peak at 442,185,927 bp also indicated
443 that SNPs across both peaks were in LD with the second peak. In both scenarios of GWAS using MLM,
444 where both peaks presented as being associated with resistance, the LD patterns were tightly linked and

Table 1. SNP-trait associations for resistance to scald using DLA BLUPs (using winter survival, heading date and plant height as covariates in the BLUPs), 374 lines and 14,789 SNPs in the MLM, MLMM, FarmCPU and BLINK GWAS models using a threshold of $-\log_{10}(p) > 4.0$.

SNP Marker Name	Chromosome	Position (bp)[a]	*p-value*	MAF[b]	Allele	Effect[c]	Phenotype Variance Explained (%)
MLM							
JHI-Hv50k-2016-168548	3	174,868,558	1.00×10^{-07}	0.465	c/t	-0.0388	14.6
SCRI_RS_221644	3	442,185,927	2.21×10^{-07}	0.471	a/g	-0.0370	0.0
JHI-Hv50k-2016-183351	3	442,550,473	4.95×10^{-07}	0.473	c/t	-0.0358	7.1
JHI-Hv50k-2016-183832	3	446,494,722	$6.75 \times 10\text{-}^{07}$	0.472	t/a	-0.0354	7.4
JHI-Hv50k-2016-183828	3	446,498,335	7.21×10^{-07}	0.476	t/c	-0.0354	7.0
MLMM							
JHI-Hv50k-2016-168548	3	174,868,558	2.57×10^{-11}	0.465	c/t	-0.0400	22.0
JHI-Hv50k-2016-514374	7	443,811,200	9.90×10^{-05}	0.326	g/k/n	-0.0434	24.1
FarmCPU							
SCRI_RS_221644	3	442,185,927	1.55×10^{-15}	0.471	a/g	-0.0320	22.4
JHI-Hv50k-2016-70026	2	18,144,891	6.76×10^{-06}	0.425	g/a	-0.0120	0.0
JHI-Hv50k-2016-202358	3	553,288,836	9.74×10^{-06}	0.300	t/c	0.0155	15.6
JHI-Hv50k-2016-232214	4	22,416,684	1.20×10^{-05}	0.240	a/t	0.0129	2.2
JHI-Hv50k-2016-514374	7	443,811,200	7.11×10^{-05}	0.326	g/t	-0.0308	0.0
BLINK							
SCRI_RS_221644	3	442,185,927	1.85×10^{-20}	0.471	a/g	-0.0351	7.3
JHI-Hv50k-2016-514374	7	443,811,200	6.54×10^{-10}	0.326	g/t	-0.0481	6.8
JHI-Hv50k-2016-202358	3	553,288,836	2.97×10^{-06}	0.300	t/c	0.0163	2.7
JHI-Hv50k-2016-232214	4	22,416,684	4.08×10^{-06}	0.240	a/t	0.0129	3.3

[a] SNP position based on Morex version 3 (Mascher et al., 2021)

[b] MAF, minor allele frequency

[c] Effect is based on Box Cox transformed data and as a result is a) not directly transferrable to unit measurements of DLA and b) the negative Box Cox transformation of DLA results in the reverse effect direction of the DLA effect.

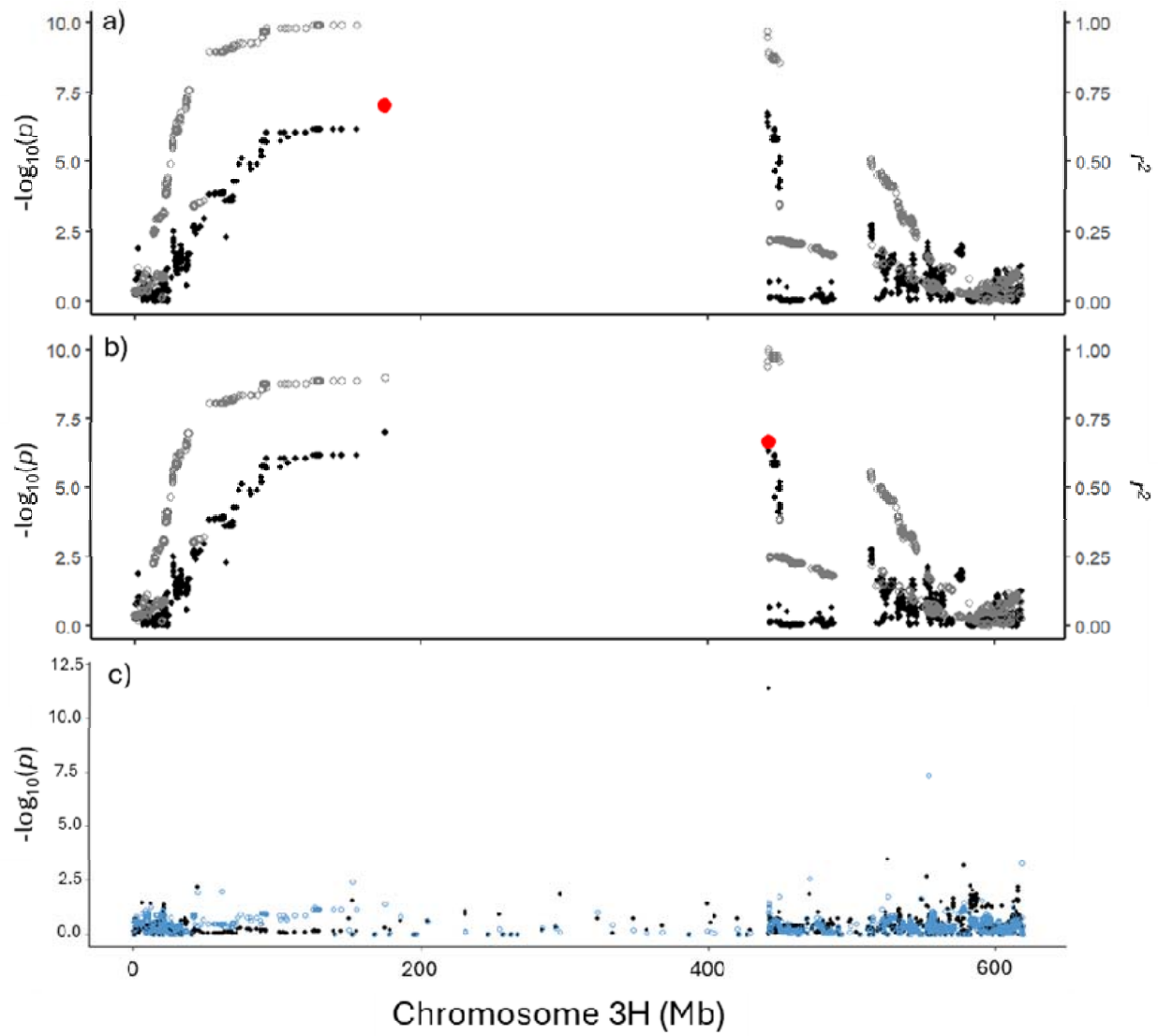

Figure 4. Dissection of the SNP-trait association cluster on chromosome 3H for resistance to scald DLA, where a) characterizes linkage disequilibrium (LD) in relation to the MLM SNP trait association at 174 Mbp, b) characterizes LD in relation to the MLM SNP-trait association at 442 Mbp. SNP associations are labeled as black dots. Linkage disequilibrium indicated as r^2 is shown in grey dots in a) and b). The most significant SNP-trait association at 174 Mbp and 442 Mbp chromosome 3H is indicated as a red dot. The FarmCPU SNP associations (c) across chromosome 3H characterizes associations across chromosome 3H in black dots. Associations using the HVS3 (*Rrs1*) SCAR marker as a covariate (c) in blue dots indicates the presence of *Rrs1* at 442 Mbp, and reveals an association at 553Mbp.

460 in coordination with the *p*-values of the surrounding SNP association landscape. As this population is
461 derived from RILs and/or DHs, it appears that the two large peaks on chromosome 3H comprise one
462 large linkage block that spans the centromere. The SNP at 442 Mbp is also the most significant SNP
463 identified via GWAS MLM, and in FarmCPU and BLINK, with FarmCPU indicating the most variation
464 explained by this SNP.

465 **3.3.2 *Rrs1* is segregating in a large linkage block on chromosome 3H**

466 The cluster of SNPs with high marker-trait associations on chromosome 3H co-localized near the *Rrs1*
467 locus. To determine if the resistance in this region is due to the major resistance gene complex, *Rrs1*, the
468 population was scored for the HVS3 SCAR marker, located downstream of the *Rrs1* gene (Genger et al.,
469 2003). 'Lightning' harbored the resistance allele at 250 bp, while 'Flavia', 'KWS Scala', 'SY Tepee' and
470 'WintMalt' carried the susceptible allele at ~500 bp. (Supplemental Table S8). The HVS3 marker was
471 used as a covariate in a FarmCPU GWAS analysis in GAPIT version 3 with 354 lines (Supplemental Tables
472 S9 & S10). The Manhattan plot along chromosome 3H (Figure 4c) indicates the presence of the SNP at
473 442 Mbp without the HVS3 SCAR marker as a covariate, and the absence of the same SNP association
474 when the HVS3 SCAR marker is used as a covariate, indicating the resistance identified via GWAS model
475 is conferred via *Rrs1*. In addition, the use of the HVS3 SCAR marker as a covariate in FarmCPU GWAS
476 model revealed the SNP association at 553 Mbp in this subset of lines, validating the second SNP on
477 chromosome 3H.

478 Based on the Morex version 3 genome, the SNP at 442,185,927 bp was located within a receptor-like
479 kinase (HORVU.MOREX.r3.HG0281210.1), that is one of several kinase and receptor-like kinase genes
480 clustered in the region. The SNP located on chromosome 3H at 553,288,836 bp co-localized with the
481 *Rrs4* gene (Patil et al., 2003), located at 576.6 Mbp. The SNP resides in a Protein 1Q-Domain 1 gene
482 (HORVU.MOREX.r3.3HG0303590.1). The *Rrs17* resistance gene is located at 10.4 Mbp (Wagner et al.,

483 2008), upstream of the SNP identified on chromosome 2H located at 18.1 Mbp, that is located within a
484 leucine-rich repeat receptor-like protein kinase (HORVU.MOREX.r3.2HG0104570). The identified SNP on
485 chromosome 4H at 22,416,684 bp is located within HORVU.MOREX.r3.4HG0338290, a glucan endo-1 3-
486 beta glucosidase gene. The SNP association on chromosome 7H at 443,811,200 is located within
487 HORVU.MOREX.r3.7HG0707540, a glycosyltransferase gene.

488 Four GWAS models were used to validate SNP associations across the genome for resistance to scald. All
489 four models have different approaches for estimating associations and are available to avoid overfitting
490 analysis. The most significant SNP association(s) in this study resided on chromosome 3H at either 174.8
491 Mbp or 422.2 Mbp. FarmCPU and Blink associations at these peaks had the lowest *p*-values (i.e., the
492 most significant) across the models. Importantly, the PVE differed between the models for these two
493 SNPs. The PVE at 174.8 Mbp ranged from 14.6% to 22.0% for MLM and MLMM, respectively. The PVE at
494 442.2 Mbp was 0.0%, 22.4% and 7.3% for the MLM, FarmCPU and BLINK models, respectively. The
495 FarmCPU model PVE of 22.4% is indicative of major gene resistance such as *Rrs1*. The SNP association
496 on chromosome 6H, explained 62.3% of the phenotypic variation in BLINK despite the very low MAF
497 (0.004) and given the variation in the few SNPs at this locus, appears to be a Type I error. The FarmCPU
498 model constrains the PVE of this SNP at 0.0%. Due to the PVE allocated for the *Rrs1* region, the
499 additional SNPs across the genome such as that on chromosome 3H at 553 Mbp, the lesser PVE of the
500 aberrant SNP on chromosome 6H, and for simplicity, the FarmCPU was the model that was used in the
501 further analysis, being considered the best fit for this population. The MLM model was also used for
502 reference.

503 **3.3.3 GWAS for resistance to scald compared to agronomic traits via FarmCPU**

504 Association analysis across disease and agronomic traits for the 374 lines was used to identify SNP
505 associations for resistance to scald, winter survival, heading date and plant height to determine if there

506 was any colocalization of marker associations that explained the phenotypic traits (Table 2;
507 Supplemental Tables S11 - 18). The BLUPs were estimated as mentioned above and included the scald
508 DLA BLUP estimate (without using the WS, HD, or HT as covariates). The QQ plots for the FarmCPU
509 analysis (Figure 5) indicated an adherence of the observed to expected $-\log_{10}(p)$ values except for several
510 SNPs at the tail of the slope, as expected. The separation of the observed to expected levels at the
511 thresholds for each of the traits was analyzed separately, and based on the Q plots, a $-\log_{10}(p) = 4.0$ was
512 used as the threshold for each trait (Figure 5).

513 DLA: In general, the SNP associations identified using the scald DLA BLUPs (without the agronomic traits
514 as covariates) using FarmCPU (Figure 5; Table 2) were similar to the previous identified SNPs (using the
515 agronomic traits as covariates; Table 1). The SNP associations on chromosome 3H included the main
516 association at 442,185,927 bp (PVE=29.4%). The same SNP associations were identified on
517 Chromosome 2H and 4H, with slightly adjusted PVE of 1.8% and 4.8%, respectively. The SNP association
518 aberrations identified in the previous analysis were also identified in this analysis and not considered for
519 further discussion based on low MAF and exaggerated PVE for the SNP on Chromosome 6H.

520 Winter Survival: A SNP association was identified on Chromosome 2H, at 4,217,244 bp (MAF = 0.432;
521 PVE = 0.8%). Additional SNPs were identified in FarmCPU including SNPs on chromosome 1H at
522 9,315,052 bp (MAF = 0.161; PVE = 5.8%), chromosome 5H at 84,325,845 bp (MAF = 0.318; PVE = 0.3%),
523 and chromosome 3H at 563,918,935 bp (MAF = 0.353; PVE = 1.8%).

524 Heading date: Of the nine SNP associations for heading date, the most significant association co-
525 localized at *Ppd-H1* (Turner et al., 2005), on chromosome 2H at 26,107,957 (MAF = 0.389; PVE = 14.0%).
526 The SNP association with the second highest PVE was located on Chromosome 1H at 417,457,946 bp
527 (MAF = 0.340; PVE = 4.7%). Similar to WS, a SNP associations were identified on chromosome 1H at
528 9,315052 (MAF = 0.161; PVE = 0.0%). The remaining SNP associations contributed <0.1% PVE.

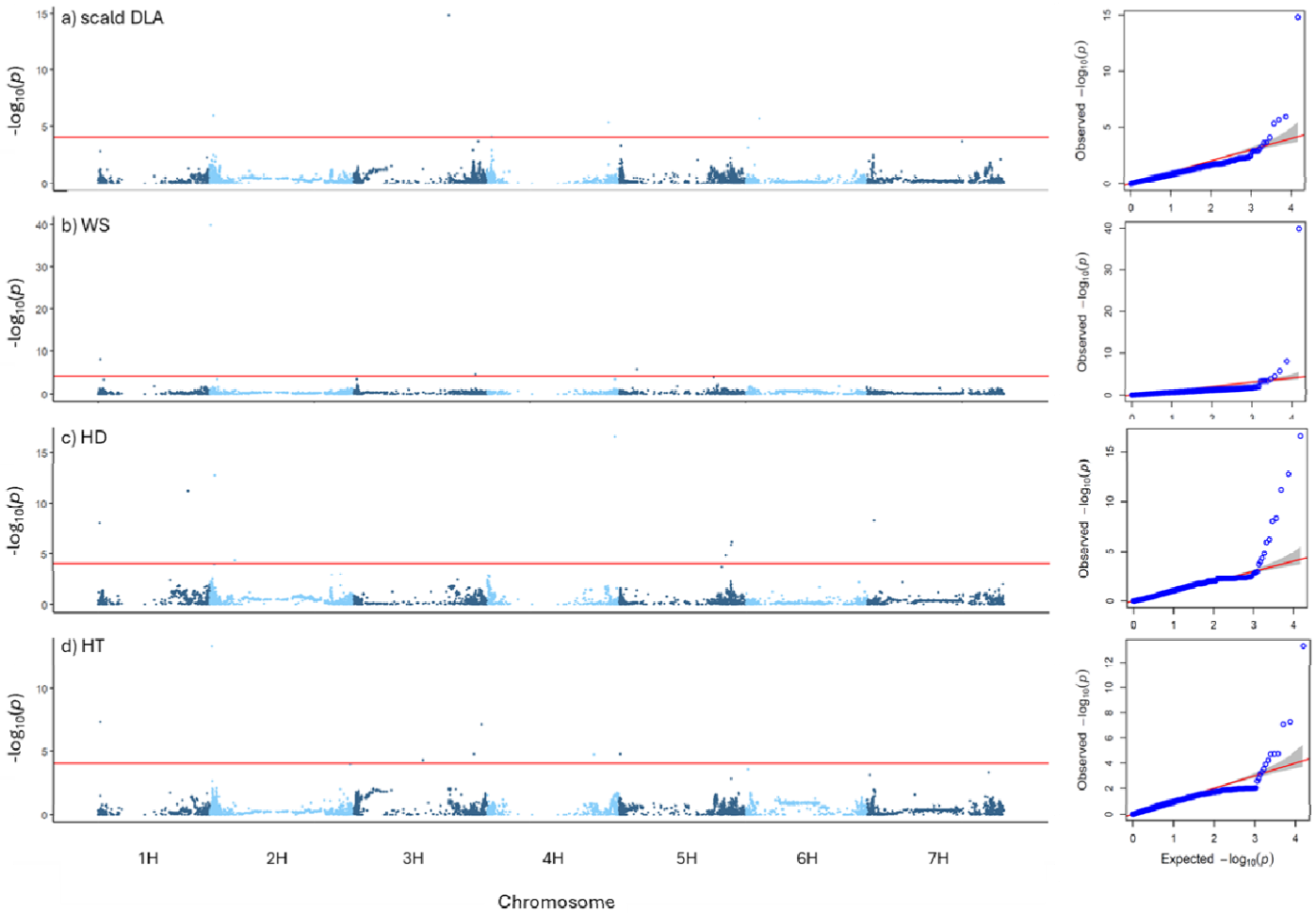

Figure 5: Manhattan plots for a) resistance to scald (DLA), b) winter survival (WS), c) heading date (HD), and d) plant height (HT) using the 374 lines and 14,789 SNPs in the FarmCPU GWAS model, and corresponding QQ plots (right). DLA BLUPs for resistance to scald were calculated without using winter survival, heading date and plant height as covariates in the BLUP model. All traits BLUPs were calculated in four environments across 2022 and 2023. The red horizontal line indicates the QQ plot – determined threshold of $-\log_{10}(p)$ of 4.0.

534 Plant Height: Seven SNP associations were identified for HT (Table 1). The most significant SNP,
535 chromosome 2H: 10,011,392 (MAF = 0.288) contributed approximately 10.7% to the phenotypic
536 variation and is localized upstream of *Ppd-H1* and the SNP association peak identified for heading date.
537 A SNP association on chromosome 1H was located at 8,999,409 bp (MAF = 0.391; PVE = 4.1%), just
538 upstream of the associations identified for winter survival and heading date. Two SNPs were associated
539 on chromosome 3H, located at 5995,758,77 bp (MAF = 0.426; PVE = 7.4%) and 560,042,502 bp (MAF =
540 0.342; PVE = 1.4%). Additional SNP associations were identified on chromosome 3H, 4H and 5H that
541 accounted for PVE from 0.0 to 5.5%,.

542 The *HvGA20ox2* gene, also known as *sdw1*, is located on chromosome 3H at 563.9 Mbp and, in previous
543 GWAS studies, was suggested to contribute towards reaction of barley to scald (Looseley et al., 2018). In
544 our study, two SNP associations for plant height were located within this region at 560.0 Mbp and 595.7
545 Mbp . The multiparent population and parental lines were genotyped using the *sdw1.d* and *sdw1.c*
546 markers (Xu et al., 2017), all of which carried the wild type allele at sdw1.

547 The correlation between resistance to scald and agronomic traits resulted in the co-localization of GWAS
548 SNP associations. The inclusion of agronomic traits in the DLA BLUPs as covariates in the initial analysis
549 (Table 1; Figure 3) appeared to slightly lower the *p*-values for identified SNP associations and resulted in
550 a higher significance threshold in comparison to DLA BLUPs without covariates, with the exception of the
551 SNP association linked to *Rrs1*. The scald DLA association identified at 553.3 Mbp on chromosome 3H,
552 was only identified when the agronomic traits were used as covariates in the scald DLA BLUPs, likely due
553 to the plant height associations found in the region. There were distinct SNP associations on the short
554 arm of chromosome 2H for resistance to scald (chromosome 2H: 18.1 Mbp; Figure 6), winter survival
555 (chromosome 2H: 4.2 Mbp), heading date (chromosome 2H; 26.1 Mbp) and plant height (chromosome
556 2H: 10.1 Mbp), however there appeared to be little genomic overlap between these peaks, as seen in
557 the Manhattan plots for the GWAS MLM model (Supplemental Fig S4). The linkage disequilibrium

558 Table 2. SNP-trait associations for diseased leaf area for scald, winter survival, heading date and plant height BLUPs, for the 374 lines and 14,789
559 SNPs in the FarmCPU GWAS model using a threshold of $-\log_{10}(p) > 4.0$. using the FarmCPU model.

SNP	Chromosome	Position (bp) [a]	*p-value*	MAF[b]	Allele	Effect[c]	Phenotype Variance Explained(%)
Scald DLA							
SCRI_RS_221644	3	442,185,927	1.48×10^{-15}	0.471	a/g	-0.0328	29.4
JHI-Hv50k-2016-70026	2	18,144,891	1.14×10^{-06}	0.425	g/a	-0.0145	1.8
JHI-Hv50k-2016-232214	4	22,416,684	7.98×10^{-05}	0.240	a/t	0.0103	4.8
Winter survival							
JHI-Hv50k-2016-61826	2	4,217,244	1.41×10^{-40}	0.432	a/g	-39533.6	0.8
JHI-Hv50k-2016-9518	1	9,315,052	9.45×10^{-09}	0.161	g/a	-17465.1	5.8
JHI-Hv50k-2016-293098	5	84,325,845	1.90×10^{-06}	0.318	c/t	22356.3	0.3
SCRI_RS_103215	3	563,918,935	3.61×10^{-05}	0.353	a/g	-9924.2	1.8
Heading date							
JHI-Hv50k-2016-267990	4	592,022,994	2.41×10^{-17}	0.395	c/t	-0.4673	0.1
JHI-Hv50k-2016-73663	2	26,107,957	1.70×10^{-13}	0.389	g/t	0.7865	14.0
SCRI_RS_231735	1	417,457,946	7.00×10^{-12}	0.340	c/a	0.3784	4.7
JHI-Hv50k-2016-456393	7	31,220,855	4.88×10^{-09}	0.150	g/t	-0.4118	0.0
JHI-Hv50k-2016-9518	1	9,315,052	9.34×10^{-09}	0.161	a/g	-0.3727	0.0
JHI-Hv50k-2016-332486	5	522,212,970	6.81×10^{-07}	0.361	t/a	-0.3034	0.0
JHI-Hv50k-2016-331267	5	519,940,617	1.34×10^{-06}	0.200	a/g	-0.3209	0.0
JHI-Hv50k-2016-320694	5	496,625,681	1.59×10^{-05}	0.367	a/g	-0.2620	2.7
JHI-Hv50k-2016-88794	2	117,994,190	5.03×10^{-05}	0.216	a/c	-0.5310	1.0
Plant height							
JHI-Hv50k-2016-64130	2	10,119,392	4.81×10^{-14}	0.288	g/r	0.0661	10.7
JHI-Hv50k-2016-9209	1	8,999,409	5.21×10^{-08}	0.391	c/t	0.0304	4.1
JHI-Hv50k-2016-216732	3	595,758,747	8.50×10^{-08}	0.426	a/c	-0.0441	7.4
SCRI_RS_150944	3	560,042,502	1.79×10^{-05}	0.342	t/c	-0.0201	1.4
JHI-Hv50k-2016-281309	5	9,453,080	1.87×10^{-05}	0.465	c/t	-0.0178	5.5
JHI-Hv50k-2016-250342	4	494,857,832	1.94×10^{-05}	0.198	g/r	0.0386	0.0
JHI-Hv50k-2016-175127	3	322,820,460	5.94×10^{-05}	0.499	n/y	-0.3041	3.8

560 [a] SNP position based on Morex version 3 (Mascher et al., 2021)
561 [b] MAF, minor allele frequency
562 [c] Effect is based on Box Cox transformed data and as a result is a) not directly transferrable to unit measurements of traits and b) the negative Box
563 Cox transformation of DLA and HD results in the reverse effect direction of effects.

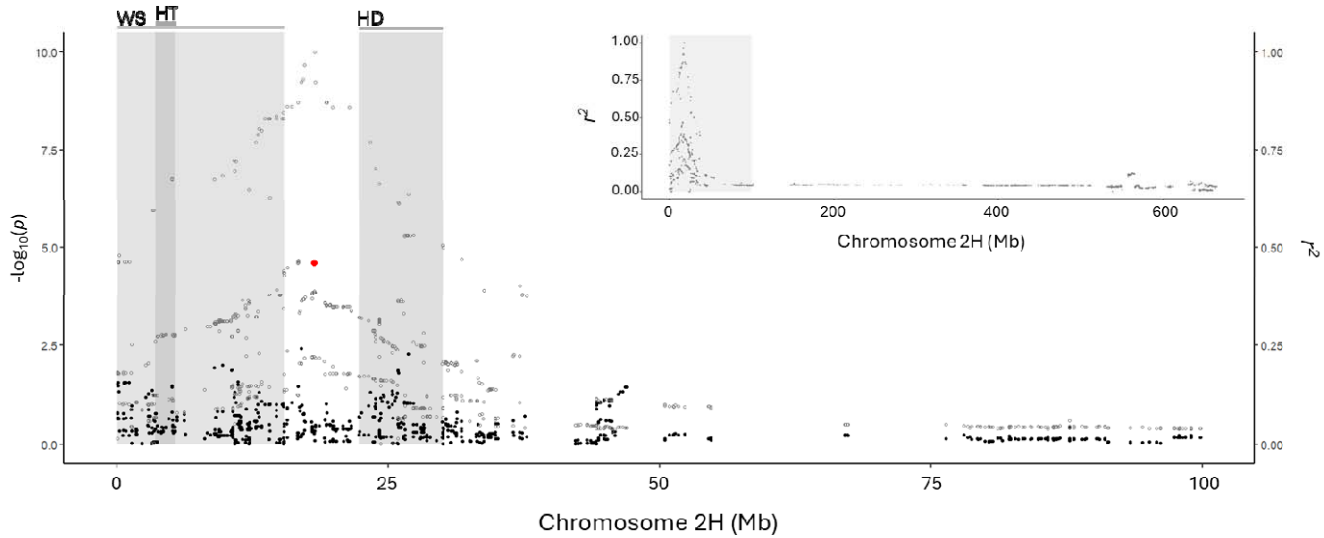

564

565 Figure 6. Association and linkage disequilibrium (LD) analysis across chromosome 2H for resistance to scald (DLA; black dots). The Manhattan
566 plot (left y axis) with black dots depicts the SNP associations for resistance to diseased leaf area (DLA) using FarmCPU in GAPIT version 3 with the
567 most significant SNP association identified as a red dot across the first 1 Mbp of chromosome 2H. Grey vertical shaded regions in the main graph
568 represent confidence intervals based on significant MLM associations (Supplemental Figure S) of co-localized SNP-trait association clusters for
569 winter survival (left, grey bar), heading date (right, grey bar) and plant height (left, dark grey bar). The LD estimate scatter plot (right *y*-axis) with
570 grey dots indicates the LD of neighboring SNPs in relation to the SNP associated with resistance to scald (in red). The top right graph insert
571 indicates the LD across chromosome 2H with respect to the most significant associated SNP for DLA. The vertical grey shaded box indicates the 1
572 Mbp region shown in the main graph.

573 between the significant peak for resistance to scald (DLA) and the remaining SNPs along chromosome 2H
574 indicated that this region may harbor LD, and that the scald DLA association should likely be considered a
575 QTL related to architectural avoidance (Figure 6). Alternatively, the SNP association is located within a
576 gene encoding agmatine coumaroyltransferase-2 (ACT-2), known to produce antifungal compounds
577 (Burhenne et al., 2003). The resistance gene, *Rrs17*, is also located at 10.4 Mbp (Wagner et al., 2008).

578 **4 DISCUSSION**

579 4.1. Breeding for resistance to scald in winter malting barley is important.

580 Malting barley is a commercially important crop due to its value in the brewing and distilling industries.
581 The malting process demands uniformly high quality grain. Winter malting barley, grown in New York for
582 the craft brewing industry, faces unique challenges due to the wet humid weather in this region. Foliar
583 fungal diseases affect both spring and winter malting barley, resulting in yield loss and kernel quality
584 issues. The environmental conditions encountered by winter malting barley grown in New York are more
585 conducive to scald infections than spring barley, even when grown in similar regions (Kolkman et al.,
586 2025a, b).

587 In this study, ambient inoculum of *R. graminicola* was relied upon for field infections. Winter malting
588 barley is planted in the fall and develops in the early spring season in New York when weather is
589 favorable for development, reaching levels of up to 77% severity in susceptible germplasm (Kolkman et
590 al., 2025a). The distribution of the susceptible parent check, 'KWS Scala', across each of the
591 environments in this study validated the consistent natural infection across the experiment, while early
592 season infections in 'KWS Scala' provided spore production across the experiment that resulted in
593 consistent disease severity in highly susceptible genotypes.

594 4.2 Resistance in the multiparent population is comprised of both major resistance genes and
595 quantitative disease resistance.

596 The *Rrs1* gene complex is an important source of resistance to scald. We identified a large linkage block
597 on chromosome 3H that spanned the centromere and initially appeared as two separate peaks in the
598 MLM GWAS model. Linkage disequilibrium analysis validated that the large region was in LD with the
599 most significant peak that co-localized near the *Rrs1* gene complex. Additional evidence of the large
600 linkage blocks was seen in the deviation of the observed: expected *p*-values as seen by the heavily
601 skewed slope in the QQ plots for the MLM model. The evidence of a large linkage block at *Rrs1* has been
602 seen in previous GWAS studies, where a large linkage block was identified on chromosome 3H for
603 seedling resistance in a diversity panel of spring barley (Hiddar et al., 2023) which was accompanied by
604 QQ plots that showed a large deviation from the expected, and where there were two peaks in LD that
605 spanned the centromeric region (Kunze et al., 2024).

606 Fine-mapping *Rrs1* to a 0.8 cM has identified ten candidate genes, however the *Rrs1* allele is in a
607 centromeric region with high linkage disequilibrium and is not present in the reference Morex genome
608 (Looseley et al., 2020). Further association analysis derived three markers near a protein kinase gene,
609 indicating the *Rrs1* may be an allelic a member of the protein kinase gene family (Looseley et al., 2020).
610 Examination of the mode of action of the *Rrs1* gene upon infection reveals that the resistance is
611 incomplete, but that hyphal development is restricted, random in the direction of growth, and exhibits a
612 delay in the collapse of the epidermal layer (Thirugnanasambandam et al., 2011). Additionally, marker
613 trait associations on chromosome 3H have been found to contribute ~27 to 30% of the phenotypic
614 variation for scald (Kunze et al., 2024; Noe et al., 2025), similar to the 22.4 – 29.4% phenotypic variation
615 explained at *Rrs1* in this study. Importantly, additional SNP marker trait associations were found across

616 the genome, including one that co-localized with *Rrs4* on chromosome 3H, and regions on chromosomes
617 2H, 4H, and 7H that can add to durable long term resistance.

618 ## 4.3 Agronomic traits can reduce disease infection

619 *Rhynchosporium graminicola* is a slow growing pathogen, requiring a three-week incubation period
620 between infection and lesion development. It capitalizes on the long early cold days of spring to
621 increase in spore load and infection. Agronomic variables can influence the rate of upward dispersal of
622 spores in the plant canopy. Winter survival is an important trait in crop improvement in northern
623 environments. The positive correlation between reduced plant density from poor winter survival (and
624 resulting reduced plot canopy) and reduced disease is an indicator of a microclimate and putative
625 reduced *R. graminicola* growth and/or spore load that leads to less disease. While not useful for
626 breeding purposes regarding management of scald through reduced canopy density, it is important to
627 include in GWAS models as a covariate for the phenotypic trait to improve SNP association identification.

628 Additional agronomic traits can help reduce infection. The negative correlation between heading date
629 and scald is indicative of an escape or avoidance mechanism, limiting the ability of *R. graminicola* conidia
630 to reach the upper leaves and spikes. The negative correlation between plant height and diseased leaf
631 area for scald also suggests an avoidance mechanism in plant defense, where elongative growth of plants
632 may outpace pathogen reproductive cycles thus delaying the rain splash dispersal of conidia to upper
633 leaves and glumes. The *sdw1* gene has previously been identified in GWAS for resistance to scald
634 (Loosely et al., 2018). In this study we identified SNP associations for resistance to scald as well as plant
635 height in the region of *sdw1* that may be independent of each other and/or a functional variant of *sdw1*
636 that has not been reported. In addition, a region on the short arm of chromosome 2H contributed to
637 plant height and heading date (via *Ppd-H1*) and to a lesser extent, winter survival. The SNP association in
638 this region may contribute to either plant architectural traits, and/or active resistance, however it

639 provides a target for selection. With a rapidly mutating pathogen, breeding for earlier heading date and
640 taller plants would help provide additional mechanisms for plant defense. The implications for disease
641 management as shorter plants are often selected or desired for reduced lodging should include selection
642 for resistance to scald.

643 ## 4.4 When your population is not that diverse: Selection of GWAS model for adapted
644 multiparent populations

645 GWAS is a powerful tool for discovery of trait genetic architecture within a population. The
646 identification of SNP marker trait associations can also aid in confirmation of previously identified
647 genetic elements, if the allele is segregating in the population at the appropriate frequency and
648 amplitude to be detected. Understanding the allele effect, or percent variation explained by the
649 SNP/marker trait association can have implications that are important to move forward with more basic
650 genetic studies, or in selection for breeding programs. Most GWAS studies utilize diverse genetic
651 populations for the pursuit of trait association analysis, relying on the thousands of meiotic
652 recombination events between the diverse lines to determine the precise genetic location of marker trait
653 associations. The availability of high-density genotyping platforms for breeding programs offers the
654 ability to use GWAS for crop improvement (Spindel et al., 2013). Breeding programs often cycle many
655 semi-related genetic materials through preliminary breeding trials to select a set number of lines to
656 move forward for selection. While early generation selection of specifically targeted and agronomically
657 important high heritability traits may limit the germplasm pool, the preliminary breeding trials are often
658 replicated across locations. Harnessing the power of GWAS in large breeding populations can be very
659 useful for understanding the genetic architecture of segregating traits in breeding programs.

660 The multiparent population was derived from a series of biparental crosses and presented a challenge in
661 how to separate population structure from effect. In this study, the SNP associations near *Rrs1* on

662 chromosome 3H varied from 174.9 Mbp accounted for 22.0% in MLMM), whereas the SNP association
663 at 442Mbp accounted for 0.0% (MLM), 22.4% (FarmCPU) and 7.3% (BLINK). The FarmCPU model
664 appeared to be the least likely to overfit or overamplify Type I associations in the structured population.
665 The MLM and MLMM GWAS models include both kinship and population structure whereas FarmCPU
666 includes kinship of associated markers and BLINK includes neither in their respective models. Population
667 structure and kinship are useful tools to reduce the confounding effects and to target unbiased marker
668 trait associations in large diverse populations. FarmCPU detected the largest amount of variation for
669 resistance to scald at the *Rrs1* locus on chromosome 3H, as well as additional QTL using more limited
670 kinship but not population structure.

671 Breeding for durable resistance to *R. graminicola* should encompass pyramiding a variety of mechanisms
672 to reduce the loss of yield and quality to scald. Major genes, such as *Rrs1*, provide a high level of
673 resistance and can be combined with QTLs and additional major resistance genes, especially those with
674 differing modes of action, to increase the resistance profile and decrease scald. In addition, selection for
675 agronomic traits, such as early flowering time and increased plant height can aid in limiting the vertical
676 spread of disease in the canopy and spike, in order to limit loss of quality and yield to scald.

677 **ACKNOWLEDGEMENTS**

678 The authors thank the field staff at the Cornell University Love Lab and Research Farm, and the small
679 grains field manager and crew, including David Benscher, Jason Schiller, Priscilla Thompson, Jenna Rice
680 and James Tanaka. We also thank Drs. Tyr Wieser-Hanks and Zhiwu Zhang for technical and theoretical
681 help with GAPIT version 3/FarmCPU, respectively. This research was supported by the intramural
682 research program of the U.S. Department of Agriculture, National Institute of Food and Agriculture,
683 Hatch accession #7002745, the USDA Barley Pest Initiative, and the New York State Department of
684 Agriculture and Markets.

CONFLICT OF INTEREST

The authors declare no conflict of interest

AUTHOR CONTRIBUTIONS

Judith M. Kolkman: Conceptualization; Data curation; Formal analysis; Investigation; Methodology; Visualization; Writing – original draft; Writing – review & editing.

Siim. S. Sepp: Investigation; Writing – review & editing.

Karl Kunze: Conceptualization; Investigation; Writing – review & editing.

Gary C. Bergstrom: Conceptualization; Funding acquisition; Project administration; Supervision; Writing – review & editing.

Mark E. Sorrells: Conceptualization; Funding acquisition; Project administration; Supervision; Writing – review & editing.

ORCID

Judith M. Kolkman: https://orcid.org/0000-0001-7388-7245

Siim S. Sepp: https://orcid.org/0000-0003-1181-7924

Karl H. Kunze: https://orcid.org/0000-0003-4548-1808

Gary Bergstrom: https://orcid.org/0000-0001-9613-270X

Mark E. Sorrells: https://orcid.org/0000-0002-7367-2663

SUPPLEMENTAL MATERIAL

All supplemental figures and tables are available for download upon publication.

DATA AVAILABILITY

Phenotypic data and GWAS results are available in supplemental tables; genotypic SNP dataset is available at (https://ics.hutton.ac.uk/50k)

707 **REFERENCES**

708

709 Ababa, G., Hailu, W., Shiferaw, T., Fekadu, W., & Alamerew, S. (2024). Adult-plant resistance to leaf
710 scald and net form net blotch in food barley genotypes at a hot spot location in Ethiopia.
711 *Heliyon*, *10*. https://doi.org/10.1016/j.heliyon.2024.e40529

712 Ababa, G., Kesho, A., Tadesse, Y., & Amare, D. (2023). Reviews of taxonomy, epidemiology, and
713 management practices of the barley scald (*Rhynchosporium graminicola*) disease. *Heliyon*, *9*.
714 https://doi.org/10.1016/j.heliyon.2023.e14315

715 Avrova, A., & Knogge, W. (2012). Rhynchosporium commune: A persistent threat to barley
716 cultivation. *Molecular Plant Pathology*, *13*, 986–997. https://doi.org/10.1111/j.1364-
717 3703.2012.00811.x

718 Ayesu-Offei, E. N., & Clare, B. G. (1970). Processes in the infection of barley leaves by
719 *Rhynchosporium secalis*. *Australian Journal of Biological Sciences*, *23*(2), 300-308.

720 Bayer, M.M., Rapazote-Flores, P., Ganal, M., Hedley, P.E., Macaulay, M., Plieske, J., Ramsay, L.,
721 Russell, J., Shaw, P.D., Thomas, W., & Waugh, R. (2017). Development and evaluation of a
722 barley 50k iSelect SNP array. *Frontiers in Plant Science*, *8*.
723 https://doi.org/10.3389/fpls.2017.01792

724 Beigi, S., Zamanizadeh[1], H., Razavi, M., & Zare[2], R. (2013). Genetic diversity of Iranian isolates of
725 barley scald pathogen (*Rhynchosporium secalis*) making use of molecular markers. *J. Agr. Sci.*
726 *Tech. Vol. 15,* 843-854.

727 Bjørnstad, Å., Patil, V., Tekauz, A., Marøy, A.G., Skinnes, H., Jensen, A., Magnus, H., & Mackey, J.
728 (2002). Genetics and resistance to scald (*Rhynchosporium secalis*) in barley (*Hordeum vulgare*)

729 studied by near-isogenic lines: I. Markers and differential isolates. *Phytopathology*, *92*(7), 710-
730 720.

731 Blachez, A.F., B.G.C., B.D., S.M.E. (2018). Evaluation of Fusarium head blight and foliar diseases on
732 winter malting barley varieties in New York, 2017. *Plant Disease Management Reports 12*,
733 CF028.

734 Bonferroni, C.E. (1936) Teoria statistica delle classi e calcolo delle probabilità, Pubblicazioni del R
735 Istituto Superiore di Scienze Economiche e Commerciali di Firenze.

736 Box, G.E.P., & Cox, D.R. (1964). An Analysis of Transformations. *Journal of the Royal Statistical*
737 *Society Series B: Statistical Methodology*, *26*, 211–243. https://doi.org/10.1111/j.2517-
738 6161.1964.tb00553.x

739 Bradbury, P.J., Zhang, Z., Kroon, D.E., Casstevens, T.M., Ramdoss, Y., & Buckler, E.S. (2007). TASSEL:
740 Software for association mapping of complex traits in diverse samples. *Bioinformatics*, *23*,
741 2633–2635. https://doi.org/10.1093/bioinformatics/btm308

742 Brunner, P.C., Schürch, S., & Mcdonald, B.A. (2007). The origin and colonization history of the barley
743 scald pathogen *Rhynchosporium secalis*. *Journal of Evolutionary Biology*, *20*, 1311–1321.
744 https://doi.org/10.1111/j.1420-9101.2007.01347.x

745 Burhenne, K., Kristensen, B.K., & Rasmussen, S.K. (2003). A new class of N-
746 hydroxycinnamoyltransferases: Purification, cloning, and expression of a barley agmatine
747 coumaroyltransferase (EC 2.3.1.64). *Journal of Biological Chemistry*, *278*, 13919–13927.
748 https://doi.org/10.1074/jbc.M213041200

Büttner, B., Draba, V., Pillen, K., Schweizer, G., & Maurer, A. (2020). Identification of QTLs conferring resistance to scald (*Rhynchosporium commune*) in the barley nested association mapping population HEB-25. *BMC Genomics*, *21*. https://doi.org/10.1186/s12864-020-07258-7

Clare, S.J., Çelik Oğuz, A., Effertz, K., Karakaya, A., Azamparsa, M.R., & Brueggeman, R.S. (2023). Wild barley (*Hordeum spontaneum*) and landraces (*Hordeum vulgare*) from Turkey contain an abundance of novel *Rhynchosporium commune* resistance loci. *Theoretical and Applied Genetics*, *136*, 1–14. https://doi.org/10.1007/s00122-023-04245-w

Coulter, M., Büttner, B., Hofmann, K., Bayer, M., Ramsay, L., Schweizer, G., Waugh, R., Looseley, M.E., & Avrova, A. (2019). Characterisation of barley resistance to *Rhynchosporium* on chromosome 6HS. *Theoretical and Applied Genetics*, *132*, 1089–1107. https://doi.org/10.1007/s00122-018-3262-8

Crous, P.W., Braun, U., McDonald, B.A., Lennox, C.L., Edwards, J., Mann, R.C., Zaveri, A., Linde, C.C., Dyer, P.S., & Groenewald, J.Z. (2021). Redefining genera of cereal pathogens: *Oculimacula*, *Rhynchosporium* and *Spermospora*. *Fungal Systematics and Evolution*, *7*, 67–98. https://doi.org/10.3114/fuse.2021.07.04

Daba, S.D., Horsley, R., Brueggeman, R., Chao, S., & Mohammadi, M. (2019). Genome-wide association studies and candidate gene identification for leaf scald and net blotch in barley (*Hordeum vulgare* L.). *Plant Disease*, *103*, 880–889. https://doi.org/10.1094/PDIS-07-18-1190-RE

Davis, J. J. (1919). Notes on parasitic fungi in Wisconsin. VI. *Trans. Wis. Acad. Sci. Arts. Lett*, *19*, 705-727.

Doyle, J. J., & Doyle, J. L. (1987). A rapid procedure for DNA purification from small quantities of fresh leaf tissue. *Phytochemical bulletin*, *19*, 11-15.

Eckstein, P.E., Griffith, L.J., Zhang, X.M., Turkington, T.K., Colin, M.G., Holden, S., Walkowiak, S., Brar, G.S., & Beattie, A.D. (2024). An island of receptor-like genes at the *Rrs13* locus on barley chromosome 6HS co-locate with three novel sources of scald resistance. *Theoretical and Applied Genetics*, *137*, 249. https://doi.org/10.1007/s00122-024-04746-2

Flint-Garcia, S.A., Thuillet, A.C., Yu, J., Pressoir, G., Romero, S.M., Mitchell, S.E., Doebley, J., Kresovich, S., Goodman, M.M., & Buckler, E.S. (2005). Maize association population: A high-resolution platform for quantitative trait locus dissection. *Plant Journal*, *44*, 1054–1064. https://doi.org/10.1111/j.1365-313X.2005.02591.x

Frank, A. B. (1897). Über die Zerstörung der Gerste durch einen neuen Getreidepilz. *Wochenschr Brau*, *42*, 518-20.

Genger, R. K., Brown, A. H., Knogge, W., Nesbitt, K., & Burdon, J. J. (2003). Development of SCAR markers linked to a scald resistance gene derived from wild barley. *Euphytica*, *134*(2), 149-159.

Hautsalo, J., Novakazi, F., Jalli, M., Göransson, M., Manninen, O., Isolahti, M., Reitan, L., Bergersen, S., Krusell, L., Damsgård Robertsen, C., Orabi, J., Due Jensen, J., Jahoor, A., Bengtsson, T., Veteläinen, M., Alsheikh, M., Jansen, C., Windju, S., Vangdorf, N., Jensen, J.D., Hjortshøj, R.L., Robertsen, C.D., Bengtsson, T., Åhman, I., Hilmarsson, H.S., & Sveinsson, S. (2021). Pyramiding of scald resistance genes in four spring barley MAGIC populations. *Theoretical and Applied Genetics*, *134*, 3829–3843. https://doi.org/10.1007/s00122-021-03930-y

Hayes, P., Carrijo, D.R., Filichkin, T., Fisk, S., Helgerson, L., Hernandez, J., Meints, B., & Sorrells, M.E. (2021). Registration of 'Lightning' barley. *Journal of Plant Registrations*, *15*, 407–414. https://doi.org/10.1002/plr2.20129

Hiddar, H., Rehman, S., Belkadi, B., Filali-Maltouf, A., Al-Jaboobi, M., Verma, R.P.S., Gyawali, S., Kehel, Z., & Amri, A. (2023). Identification of sources of resistance to scald (*Rhynchosporium commune*) and of related genomic regions using genome-wide association in a mapping panel of spring barley. *Frontiers in Plant Science*, *14*. https://doi.org/10.3389/fpls.2023.1133404

Huang, M., Liu, X., Zhou, Y., Summers, R.M., & Zhang, Z. (2019). BLINK: A package for the next level of genome-wide association studies with both individuals and markers in the millions. *GigaScience*, *8*. https://doi.org/10.1093/gigascience/giy154

Ijaz, U., Zhao, C., Shahbala, S., & Zhou, M. (2024). Genome-wide association study for identification of marker-trait associations conferring resistance to scald from globally collected barley germplasm. *Phytopathology*, *114*, 1637–1645. https://doi.org/10.1094/PHYTO-01-24-0043-R

Kelly, J. D., Kolkman, J. M., & Schneider, K. (1998). Breeding for yield in dry bean (*Phaseolus vulgaris* L.). *Euphytica*, *102*(3), 343-356.

Kolkman, J.M., Bergrstom, G.C., Benscher, D., & Sorrells, M.E. (2025)(a). Reaction of winter malting barley cultivars and breeding lines to foliar diseases in New York, 2024. *Plant Health Progress*, *26*, 404–404. https://doi.org/10.1094/PHP-12-24-0172-PDMR

Kolkman, J.M., Bergrstom, G.C., Benscher, D., & Sorrells, M.E. (2025)(b). Reaction of spring malting barley cultivars and breeding lines to foliar diseases in New York, 2024. *Plant Health Progress*, *26*, 405–405. https://doi.org/10.1094/PHP-12-24-0173-PDMR

Kunze, K.H., Meints, B., Massman, C., Gutiérrez, L., Hayes, P.M., Smith, K.P., Bergstrom, G.C., & Sorrells, M.E. (2024). Genome-wide association of an organic naked barley diversity panel identified quantitative trait loci for disease resistance. *Plant Genome*, *17*(4), e20530. https://doi.org/10.1002/tpg2.20530

Lehnackers, H., & Knogge, W. (1990). Cytological studies on the infection of barley cultivars with known resistance genotypes by *Rhynchosporium secalis*. *Canadian Journal of Botany*, *68*(9), 1953-1961.

Linsell, K.J., Keiper, F.J., Forgan, A., & Oldach, K.H. (2011). New insights into the infection process of *Rhynchosporium secalis* in barley using GFP. *Fungal Genetics and Biology*, *48*, 124–131. https://doi.org/10.1016/j.fgb.2010.10.001

Liu, X., Huang, M., Fan, B., Buckler, E.S., & Zhang, Z. (2016). Iterative usage of fixed and random effect models for powerful and efficient genome-wide association studies. *PLoS Genetics*, *12*. https://doi.org/10.1371/journal.pgen.1005767

Looseley, M.E., Griffe, L.L., Büttner, B., Wright, K.M., Middlefell-Williams, J., Bull, H., Shaw, P.D., Macaulay, M., Booth, A., Schweizer, G., Russell, J.R., Waugh, R., Thomas, W.T.B., & Avrova, A. (2018). Resistance to *Rhynchosporium commune* in a collection of European spring barley germplasm. *Theoretical and Applied Genetics*, *131*, 2513–2528. https://doi.org/10.1007/s00122-018-3168-5

Looseley, M.E., Ramsay, L., Bull, H., Swanston, J.S., Shaw, P.D., Macaulay, M., Booth, A., Russell, J.R., Waugh, R., & Thomas, W.T.B. (2020). Association mapping of malting quality traits in UK spring and winter barley cultivar collections. *Theoretical and Applied Genetics*, *133*, 2567–2582. https://doi.org/10.1007/s00122-020-03618-9

834 Marzin, S., Hanemann, A., Sharma, S., Hensel, G., Kumlehn, J., Schweizer, G., & Röder, M.S. (2016).
835 Are pectin esterase inhibitor genes involved in mediating resistance to *Rhynchosporium*
836 commune in barley?. *PLoS ONE*, *11*(3), e0150485.
837 https://doi.org/10.1371/journal.pone.0150485

838 Mascher, M., Gundlach, H., Himmelbach, A., Beier, S., Twardziok, S.O., Wicker, T., Radchuk, V.,
839 Dockter, C., Hedley, P.E., Russell, J., Bayer, M., Ramsay, L., Liu, H., Haberer, G., Zhang, X.Q.,
840 Zhang, Q., Barrero, R.A., Li, L., Taudien, S., Groth, M., Felder, M., Hastie, A., Šimková, H.,
841 Stanková, H., Vrána, J., Chan, S., Munõz-Amatriaín, M., Ounit, R., Wanamaker, S., Bolser, D.,
842 Colmsee, C., Schmutzer, T., Aliyeva-Schnorr, L., Grasso, S., Tanskanen, J., Chailyan, A., Sampath,
843 D., Heavens, D., Clissold, L., Cao, S., Chapman, B., Dai, F., Han, Y., Li, H., Li, X., Lin, C., McCooke,
844 J.K., Tan, C., Wang, P., Wang, S., Yin, S., Zhou, G., Poland, J.A., Bellgard, M.I., Borisjuk, L.,
845 Houben, A., Doleael, J., Ayling, S., Lonardi, S., Kersey, P., Langridge, P., Muehlbauer, G.J., Clark,
846 M.D., Caccamo, M., Schulman, A.H., Mayer, K.F.X., Platzer, M., Close, T.J., Scholz, U., Hansson,
847 M., Zhang, G., Braumann, I., Spannagl, M., Li, C., Waugh, R., & Stein, N. (2017). A chromosome
848 conformation capture ordered sequence of the barley genome. *Nature*, *544*, 427–433.
849 https://doi.org/10.1038/nature22043

850 Mascher, M., Wicker, T., Jenkins, J., Plott, C., Lux, T., Koh, C.S., Ens, J., Gundlach, H., Boston, L.B.,
851 Tulpová, Z., Holden, S., Hernández-Pinzón, I., Scholz, U., Mayer, K.F.X., Spannagl, M., Pozniak,
852 C.J., Sharpe, A.G., Simková, H., Moscou, M.J., Grimwood, J., Schmutz, J., & Stein, N. (2021).
853 Long-read sequence assembly: A technical evaluation in barley. *Plant Cell*, *33*, 1888–1906.
854 https://doi.org/10.1093/plcell/koab077

855 Mcdonald, B.A. (2015). How can research on pathogen population biology suggest disease
856 management strategies? The example of barley scald (*Rhynchosporium commune*). *Plant*
857 *Pathology*, *64*, 1005–1013. https://doi.org/10.1111/ppa.12415

858 Noe, S.M., Åstrand, J., Zakieh, M., Singh, P.K., Johansson, E., & Chawade, A. (2025). Harnessing
859 novel genetic markers for scald resistance from gene bank spring barley genotypes. *BMC Plant*
860 *Biology*, *25*(1), 781. https://doi.org/10.1186/s12870-025-06813-2

861 Patil, V., Bjørnstad, Å., & Mackey, J. (2003). Molecular mapping of a new gene Rrs4 CI 11549 for
862 resistance to barley scald (*Rhynchosporium secalis*). *Molecular Breeding*, *12*(2), 169-183.

863 Ryan, C.C., & Grivell, C.J. (1974). An Electron Microscope Study of the Outer Layers of Barley Leaves
864 Infected with *Rhynchosporium secalis*. *Aust. J. Plant Physiol*

865 Segura, V., Vilhjálmsson, B.J., Platt, A., Korte, A., Seren, Ü., Long, Q., & Nordborg, M. (2012). An
866 efficient multi-locus mixed-model approach for genome-wide association studies in structured
867 populations. *Nature Genetics*, *44*, 825–830. https://doi.org/10.1038/ng.2314

868 Shipton, W. A., Boyd, W. J. R., & Ali, S. M. (1974). Scald of barley. 839-861.

869 Shrestha, R.K., & Lindsey, L.E. (2019). Agronomic management of malting barley and research
870 needs to meet demand by the craft brew industry. *Agronomy Journal*, *111*, 1570–1580.
871 https://doi.org/10.2134/agronj2018.12.0787

872 Siller, A., Hashemi, M., Wise, C., Smychkovich, A., & Darby, H. (2021). Date of planting and nitrogen
873 management for winter malt barley production in the northeast, USA. *Agronomy*, *11*.
874 https://doi.org/10.3390/AGRONOMY11040797

875 Spindel, J., Wright, M., Chen, C., Cobb, J., Gage, J., Harrington, S., Lorieux, M., Ahmadi, N., &
876 McCouch, S. (2013). Bridging the genotyping gap: Using genotyping by sequencing (GBS) to

add high-density SNP markers and new value to traditional bi-parental mapping and breeding populations. *Theoretical and Applied Genetics*, *126*, 2699–2716. https://doi.org/10.1007/s00122-013-2166-x

Thirugnanasambandam, A., Wright, K.M., Atkins, S.D., Whisson, S.C., & Newton, A.C. (2011). Infection of *Rrs1* barley by an incompatible race of the fungus *Rhynchosporium secalis* expressing the green fluorescent protein. *Plant Pathology*, *60*, 513–521. https://doi.org/10.1111/j.1365-3059.2010.02393.x

Tibbs Cortes, L., Zhang, Z., & Yu, J. (2021). Status and prospects of genome-wide association studies in plants. *Plant Genome*, *14*(1), e20077. https://doi.org/10.1002/tpg2.20077

Turner, A., Beales, J., Faure, S., Dunford, R. P., & Laurie, D. A. (2005). The pseudo-response regulator *Ppd-H1* provides adaptation to photoperiod in barley. *Science*, *310*(5750), 1031-1034.

Wagner, C., Schweizer, G., Krämer, M., Dehmer-Badani, A.G., Ordon, F., & Friedt, W. (2008). The complex quantitative barley-*Rhynchosporium secalis* interaction: Newly identified QTL may represent already known resistance genes. *Theoretical and Applied Genetics*, *118*, 113–122. https://doi.org/10.1007/s00122-008-0881-5

Wang, J., & Zhang, Z. (2021). GAPIT Version 3: Boosting Power and Accuracy for Genomic Association and Prediction. *Genomics, Proteomics and Bioinformatics*, *19*, 629–640. https://doi.org/10.1016/j.gpb.2021.08.005

Wang, Y., Xu, Y., Gupta, S., Zhou, Y., Wallwork, H., Zhou, G., Broughton, S., Zhang, X.Q., Tan, C., Westcott, S., Moody, D., Sun, D., Loughman, R., Zhang, W., & Li, C. (2020). Fine mapping QSc.VR4, an effective and stable scald resistance locus in barley (*Hordeum vulgare* L.), to a

898 0.38-Mb region enriched with LRR-RLK and GLP genes. *Theoretical and Applied Genetics*, *133*,
899 2307–2321. https://doi.org/10.1007/s00122-020-03599-9

900 Xu, Y., Jia, Q., Zhou, G., Zhang, X.Q., Angessa, T., Broughton, S., Yan, G., Zhang, W., & Li, C. (2017).
901 Characterization of the *sdw1* semi-dwarf gene in barley. *BMC Plant Biology*, *17*.
902 https://doi.org/10.1186/s12870-016-0964-4

903 Yu, J., Pressoir, G., Briggs, W.H., Bi, I.V., Yamasaki, M., Doebley, J.F., Mcmullen, M.D., Gaut, B.S.,
904 Nielsen, D.M., Holland, J.B., Kresovich, S., & Buckler, E.S. (2006). A unified mixed-model
905 method for association mapping that accounts for multiple levels of relatedness *38*, 203–208.
906 https://doi.org/10.1038/ng1702

907 Zaffarano, P.L., McDonald, B.A., & Linde, C.C. (2008). Rapid speciation following recent host shifts in
908 the plant pathogenic fungus *Rhynchosporium*. *Evolution*, *62*, 1418–1436.
909 https://doi.org/10.1111/j.1558-5646.2008.00390.x

910 Zaffarano, P.L., McDonald, B.A., & Linde, C.C. (2011). Two new species of *Rhynchosporium*.
911 *Mycologia*, *103*, 195–202. https://doi.org/10.3852/10-119

912 Zhang, X., Ovenden, B., & Milgate, A. (2020). Recent insights into barley and *Rhynchosporium*
913 *commune* interactions. *Molecular Plant Pathology*, *21*, 1111–1128.
914 https://doi.org/10.1111/mpp.12945

915 Zhang, Z., Ersoz, E., Lai, C.Q., Todhunter, R.J., Tiwari, H.K., Gore, M.A., Bradbury, P.J., Yu, J., Arnett,
916 D.K., Ordovas, J.M., & Buckler, E.S. (2010). Mixed linear model approach adapted for genome-
917 wide association studies. *Nature Genetics*, *42*, 355–360. https://doi.org/10.1038/ng.546

918

SUPPLEMENTAL FIGURES CONTENT

Figure S1. Frequency distribution for a) scald diseased leaf area, b) winter survival, c) heading date (Julian), and d) plant height shows transgressive segregation in the population of 377 lines derived from the parental lines. Values for each parental line are indicated by the blue arrows for each of the disease and agronomic traits. 'Endeavor', a check cultivar grown across blocks and experiments is also shown for comparison.

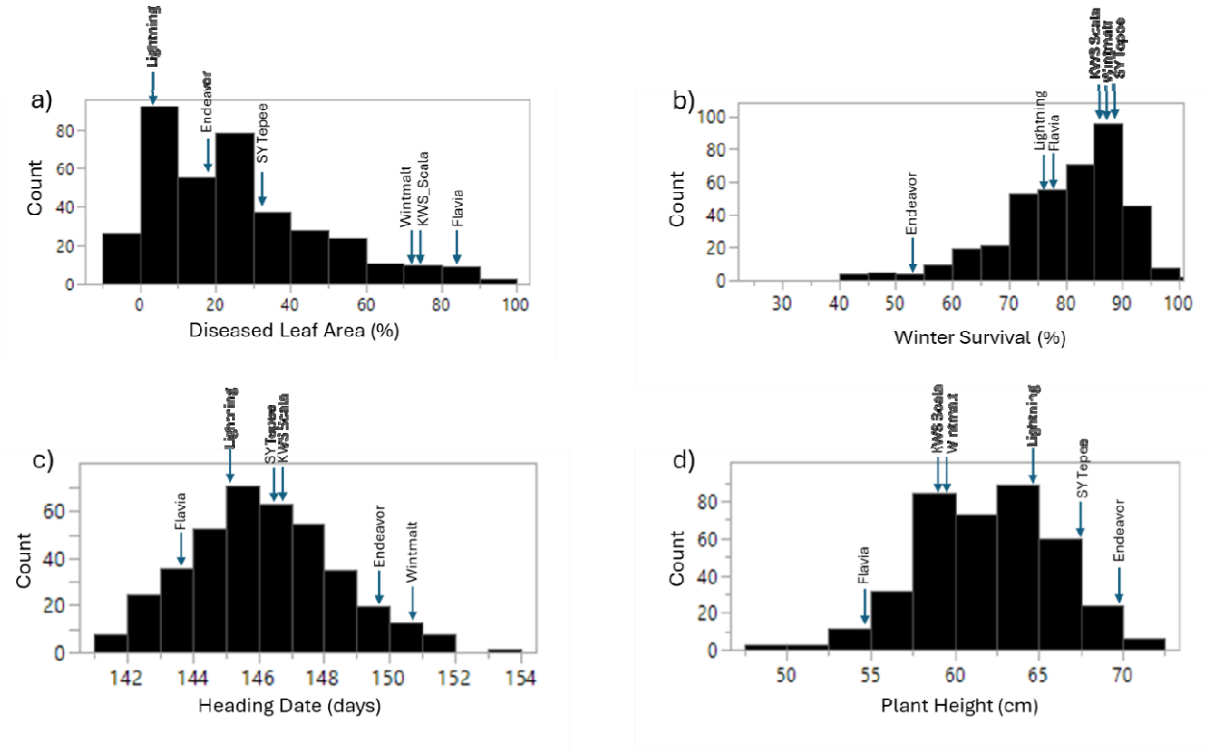

928 Figure S2. Principal component analysis for the 374 lines of the multiparent population

929 displaying a) PCA eigenvalues and b) genotype clustering for PCA = 3.

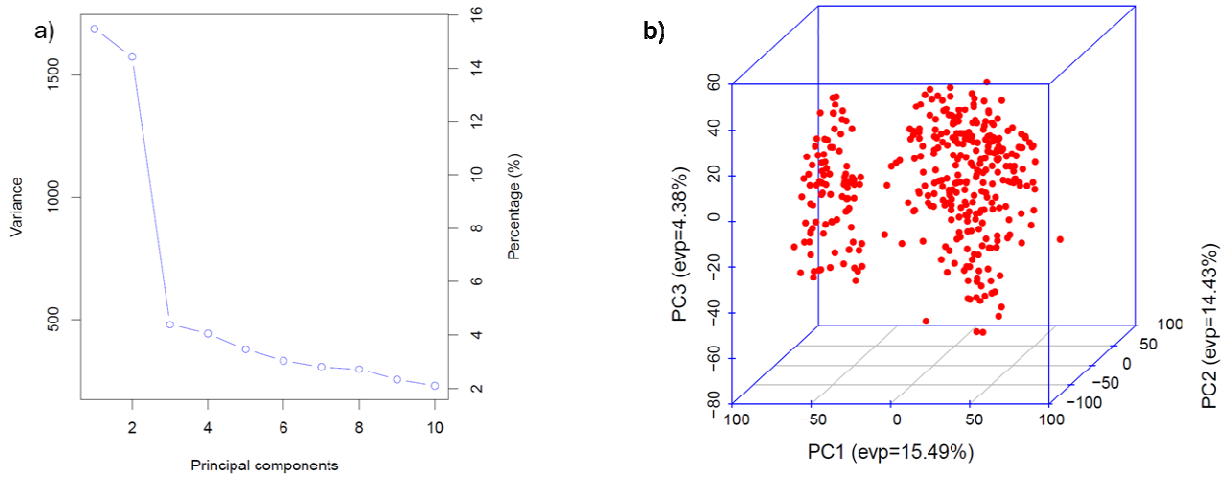

930

931

932 Figure S3. Quantile-quantile plot for FarmCPU GWAS model for resistance to scald in winter

933 malting barley using PCA=3 as a covariate.

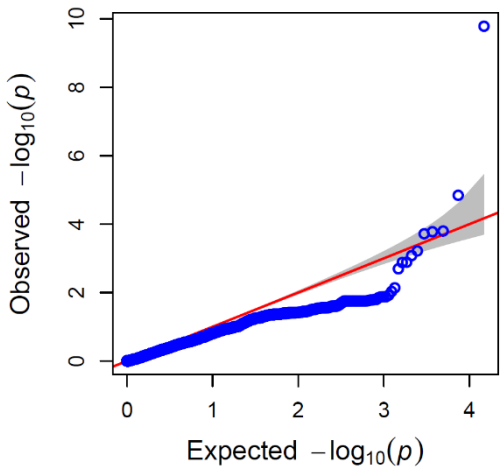

934

935

936 Figure S4: Manhattan plots for a) resistance to scald (DLA), b) winter survival (WS), c) heading date (HD), and d) plant height (HT)

937 using the 374 lines and 14,789 SNPs in the MLM GWAS mode, with corresponding QQ plots (right). DLA BLUPs for resistance to scald

938 were calculated without using WS, HD date and HT as covariates in the BLUP model. All traits BLUPs were calculated in four

939 environments across 2022 and 2023. The red horizontal line indicates the QQ plot – determined threshold of $-\log_{10}(p)$ of 4.0.

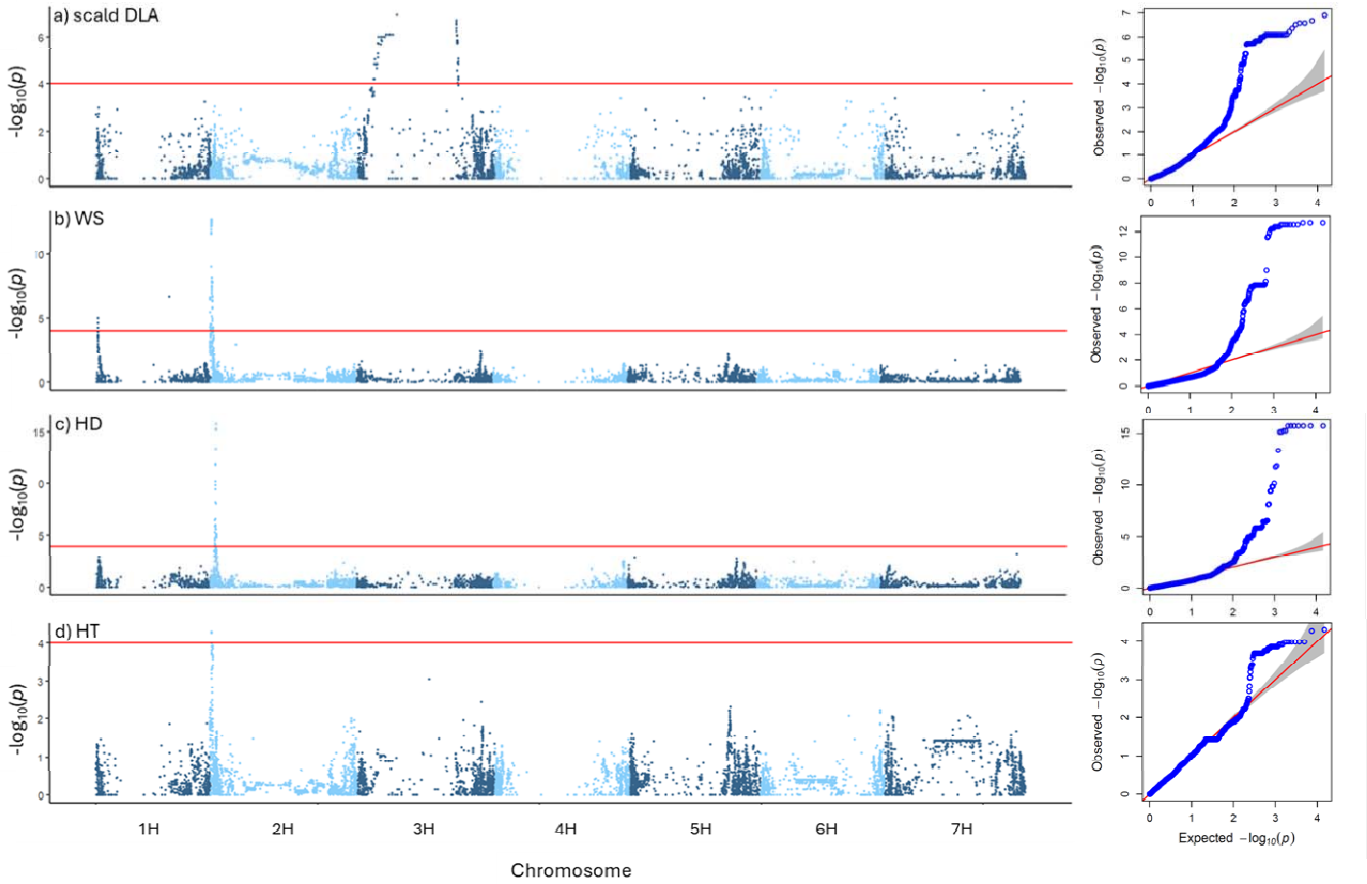

940

941 **SUPPLEMENTAL TABLES CONTENT**

942 Table S1. Diseased leaf area for scald, winter survival, heading date and plant height in the multiparent
943 population across four environments.

944 Table S2. Least square means of diseased leaf area for scald, winter survival, heading date and plant
945 height for the multiparent population across four environments.

946 Table S3. Transformed diseased leaf area BLUPs with and without agronomic covariates, as well as the
947 transformed winter survival, heading date and plant height across four environments.

948 Table S4. GWAS MLM statistics for DLA BLUPs with agronomic trait covariates

949 Table S5. GWAS MLMM statistics for DLA BLUPs with agronomic trait covariates

950 Table S6. GWAS FarmCPU statistics for DLA BLUPs with agronomic trait covariates

951 Table S7. GWAS BLINK statistics for DLA BLUPs with agronomic trait covariates

952 Table S8. HVS3 SCAR marker allele sizes linked to *Rrs1* in the multiparent population.

953 Table S9. GWAS FarmCPU statistics for DLA BLUPs on chromosome 3H with 354 line subset

954 Table S10. GWAS FarmCPU statistics for DLA BLUPs on chromosome 3H with 354 line subset and HVS3
955 covariate.

956 Table S11. GWAS MLM statistics for DLA BLUPs with no agronomic covariates

957 Table S12. GWAS FarmCPU statistics for DLA BLUPs with no agronomic covariates

958 Table S13. GWAS MLM statistics for WS BLUPs

959 Table S14. GWAS FarmCPU statistics for winter survival BLUPs

960 Table S15. GWAS MLM statistics for heading date BLUPs

961 Table S16. GWAS FarmCPU statistics for heading date BLUPs

962 Table S17. GWAS MLM statistics for plant height BLUPs

963 Table S18. GWAS FarmCPU statistics for plant height BLUPs